Wound Healing Activity of (1→3),(1→6)-β-D-Glucan and Interaction of Cells with β-glucan/PLGA composite scaffold

Yeon I Woo

Department of Medical Science

The Graduate School, Yonsei University

Wound Healing Activity of (1→3),(1→6)-β-D-Glucan and Interaction of Cells with β-glucan/PLGA composite scaffold

Directed by Professor Jong-Chul Park

The Master's Thesis
submitted to the Department of Medical Science,
the Graduate School of Yonsei University
in partial fulfillment of the requirements for the
degree of Master of Medical Science

Yeon I Woo

December 2008

This certifies that the Master's Thesis of Yeon I Woo is approved.

Thesis Supervisor : Jong-Chul Park

Dong Kyun Rah

Won Taek Lee

The Graduate School
Yonsei University

December 2008

ACKNOWLEDGEMENTS

나에게 있어서 대학원 석사 과정은 남들과 다르게 거의 3년이란 시간을 보냈기에 또 다른 의미가 있었던 시간이었습니다. 졸업이라는 시간이 다가오면서 처음 여기에 발을 들여놨을 때의 마음가짐을 되새겨 보게 됩니다. 연구생에 이어 석사과정 동안 많은 것들을 느끼고, 배우고, 많은 사람들을 만나고, 내 자신이 한 단계 성장하는 시간이었던 것 같습니다. 이 지면을 빌어 여러 고마운 분들께 감사한 마음을 전하고자 합니다.

이 논문이 완성되기까지 학문적 가르침과 조언 외에도 연구하는 사람으로서의 자세와 말썽 많은 저를 끝까지 믿고 이끌어주신 박종철 교수님께 진심으로 감사드립니다. 바쁘신 데도 불구하고 미흡한 제 논문을 처음부터 끝까지 꼼꼼하게 수정해주신 성형외과 나동균 교수님과 논문 지도를 맡아 주신 이원택 교수님께 깊이 감사드립니다. 매주 세미나 시간을 알찬 토의로 이끌어주시고 조언도 아끼지 않으시는 나노사업단의 이인섭 교수님과 세종대 이권용 교수님께도 감사의 말씀을 전합니다. 인간적으로나 학문적으로나 모법을 보여주신 김정구 교수님, 최재봉 교수님께도 감사드립니다.

3년 반이라는 시간동안 의학공학교실 일원으로 항상 함께 해준 우리 실험실원 모두에게 감사의 마음을 전하고 싶습니다. 실험에 있어서 많은 것을 알려주시는 박봉주 선생님, 지금은 부산대 교수님이 되신 한동욱 선생님, 저의 진로를 진심으로 걱정해주시고 도움주신 김정성 선생님과 임도형 박사님, 실험실 분위기 메이커~현숙언니, 다시 돌아오셔서 넘 좋아요! 혜련언니, 실험실의 큰일은 다 도맡아하는 미희, 냉정해 보여도 속은 따뜻한 혜리, 말로는 절대 못 이기는 동료/동창! 진교수 수창, 새침한 듯 안한 듯 박여사 동정, 술 먹으면 애교쟁이로 변하는 재경이, 나이는 어려도 옛날 일까지 다 아는 술친구 병주, 늘 성실하고 함박웃음 주는 대형이, 은근 된장남 깐족쟁이 장염선배 민성, 은근 엽기 좋아하는 Barbora, 멀리 미쿡에 있는 막둥이 같은

장남 진횬, 금주언니, 결혼해서 더 행복해 보이는 현주언니, PLGA에 관해 늘 도움을 주는 인제대 성미& 혁진, 아주대의 완전 재미있으신 원섭쌤& 경민쌤,

늘 나의 피와 살을 살찌우게 만드는 쑤, 정인, 짱양(너희랑 같이 마신 술값으로 건물하나 짓겠다), 늘 앓는 소리하는 미노, 15년 동안 아무 때나 콜!하면 나타나주는 영희, 이젠 그만 방황하고 한국에 왔으면 하는 명수, 나와 같이 외국생활을 꿈꾸는 선영(올해는 가자!), 꼭 10억 벌어서 나 좀 주라 상우야, 늘 주위를 밝게 해주는 주희(기채), 건조한 삶의 한 줄기 빛인 베누스토~무뚝뚝하지만 뒤에선 자상한 형 진오라버니, 피스까지 주신 민석오라버니, 계원언니..피아노학원 잘되길, 트럼펫 수석 경선언니(이번엔 꼭 합격하실꺼예요~), 엉뚱하고 호기심 많은 찬옥언니, 유포늄의 세계를 알게 해주신 호진호쌤,

한국에 오면 늘 선물과 함께 써프라이즈 해주시는 やすたかさん、일본어를 잊지 않게 도와주는 ゆきちゃん、なおみちゃん!벌써 알고지낸지 10년이나 넘었네..공연장멤버 종석이, 지영이..앞으로도 쭈욱 콘서트는 너네와 함께야~

생각하는 것만으로도 가슴 벅찬 아버지, 어머니께 사랑하는 마음 전합니다. 부족한 딸이지만 저를 믿고 제가 선택하는 길을 지지해주셔서 감사합니다. 그리고 친구 같은 언니, 요즘 사랑에 부쩍 빠져있는 영애에게도 고마운 마음 전합니다. 언제나 저에게 사랑을 듬뿍 주시는 할머니께도 감사합니다!(아프지 마셔요~!)

많은 분들의 후원과 사랑에 보답하는 마음으로 어디에서든 최선을 다하는 모습 보여드리겠습니다.

2009년 1월
우연이 드림

Contents

Figure legends

Table legends

Abbreviations

aHDFs: adult human dermal fibroblasts

ADSCs: Adipose tissue-derived mesenchymal stem cells

ECM : Extracellular matrix

DMEM : Dulbecco's modified Eagle's medium

FBS : Fetal bovine serum

PBS : Phosphate buffered saline

CCD : Charge-coupled device

NO: Nitric oxide

LPS: lipopolysaccharide

iNOS: inducible nitric oxide synthase

COX-2: cyclooxygenase-2

PGE_2: Prostaglandin E_2

Abstract

Wound Healing Activity of (1→3),(1→6)-β-D-Glucan and Interaction of Cells with β-glucan/PLGA composite scaffold

Yeon I Woo

Department of Medical Science
The Graduate School, Yonsei University

(Directed by Professor Jong-Chul Park)

β-Glucan is a natural product of glucose polymer, which has immune stimulatory activity, especially effective on wound healing. Wound healing is a highly complex physiological process that involves the interaction of various cells with diverse phenotypes such as macrophages, fibroblasts, and it is mainly mediated by immune reaction. It is generally accepted that wound healing is mediated by immune reaction and macrophage is a pivotal cell in wound repair. In actuality it has been reported that after the occurrence of wound, macrophages are activated and secrete a plethora of biologically active substances, such as nitric oxide.

In this study, we investigated the possible roles of β-glucans in skin wound healing process, especially in the aspect of adult human dermal fibroblast(aHDFs)/Adipose tissue-derived mesenchymal stem cells(ADSCs) activation-proliferation, migration and collagen gel contraction. β-glucans were tested for the ability as an anti-inflammatory factor using

lipopolysaccharide(LPS)-stimulated macrophage cell line(RAW 264.7 macrophages). Finally, a porous electrospun scaffold was prepared by physically blending β-glucans and poly lactide-co-glycolide (PLGA). The interaction between cells and the β-glucan/PLGA composite scaffold such as attachment, proliferation, and the biosafety test were characterized.

The results of the cellular responses of aHDFs/ADSCs, such as proliferation and migration, were enhanced on the β-glucans. Moreover, β-glucans inhibited LPS-stimulated expression of nitric oxide synthase induction and inducible cyclooxygenase in a concentration-dependent manner. And the results of collagen gel assay also revealed that gel contraction was enhanced by the β-glucans. Additional to those *in vitro* evidences, topical administration of β-glucan was useful to promote wound healing. Furthermore, the cellular responses of aHDFs/ADSCs, such as attachment and proliferation, were enhanced on the β-glucan/PLGA composite scaffolds. The results indicated that cells interacted favorably with the scaffold. Using an biological safety test of β-glucan/PLGA composite scaffold, experiments was also performed in vitro for test groups as used in the above test. Under the conditions of this study, the test article extract showed nontoxic compared with negative control.

In conclusion, These findings suggested that β-glucan/PLGA composite scaffold can potentially be useful in enhancing the healing of chronic or trauma wounds.

Key Words : (1→3),(1→6)-β-D-glucan, wound healing, adult human dermal fibroblasts, adipose tissue-derived mesenchymal stem cells, collagen, PLGA, scaffold

Wound Healing Activity of (1→3),(1→6)-β-D-Glucan and

Interaction of Cells with β-glucan/PLGA composite scaffold

Yeon I Woo

Department of Medical Science
The Graduate School, Yonsei University

(Directed by Professor Jong-Chul Park)

I. Introduction

1. β-D-Glucans

Glucans are polymers of glucose that are widely distributed throughout the biosphere.[1] Specifically, these glucose polymers are produced by a variety of plants, such as oat, barley, and seaweed. β-glucans are the constituents of the cell wall of certain pathogenic bacteria (*Pneumocystis carinii, Cryptococcus neoformans, Aspergillus fumigatus, Histoplasma capsulatum, Candida albicans)* and fungi *(Saccharomyces cerevisiae).* The main components of the fungal cell wall are polysaccharides and glycoproteins. Glucans can be broadly classified according to the ty pe of intrachain link age of the polymer, as α- or β-linked.[1] The β-linked glucans are the predominant form found in fungi.[1] It is the fu ngal-derived (1→3)-β-D-glucans which have been reported to modulate var ious aspects of immunity.[2-5] In the fungal cell wall, (1→3)-β-D

-glucans are linked to proteins, lipids and other carbohydrates such as m annan[1]. The specific function of glucans in the physiology of fungi is n ot clearly understood. The glucan polymers in the fungal cell wall may form a meshwork, due to the presence of (1→6)-β-D-glucopyranose side chain branches, which may connect adjacent (1→3)-β-D-glucan polymers .[1] Figure 1 shows the basic structure for a non-branched (1→3)-β -D-glucan polymer and for a (1→3)-β-D-glucan polymer with single (1→ 6)-β side-chain branches.

β-glucans are well known as a wound healing accelerator. Glucans have been demonstrated to have immune stimulatory activity, especially to enhance wound healing by increasing macrophage infiltration into the injury sites, stimulating tissue granulation, collagen deposition, and re-epithelialization.[6-9] It has been reported that topical or systemic glucan administration enhances wound healing.[6,7,10-13] Delatte et al. reported that pediatric burns can be effectively treated with β-glucan-collagen mixtures and that this preparation markedly simplified wound care and significantly decreased post-injury pain.[9] These observations suggest that β-glucans and related immunomodulators may be useful adjuncts for healing, particularly in burn wounds. Kougias et al. have reported the presence of at least two glucan binding sites on normal human dermal fibroblasts other than immunocytes like mammalian macrophages.[14] However, until now these kinds of investigations cannot have clarified the pathways of the effects of β-D-glucan on wound healing *in vitro,* and also *in vivo* systematically. Up to the present, some clinical application cases have been reported, but there are no verified explanations about how β-glucan affects on wound healing.

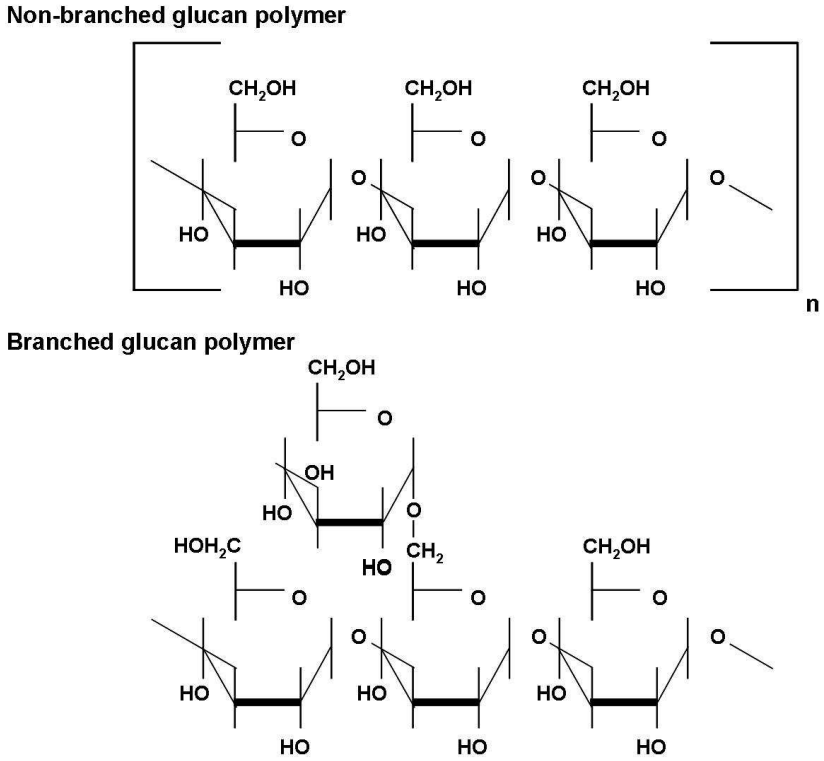

Figure 1. Primary structure of a single, non-br anched and a single, branched (1→3)-β-D-glucan polymer. The backbone of the glucan polymer is composed of glucose subunits connected by intrachain glycosidic (1→3)-β-linkages. In a branched (1→3)-β-D-glucan polymer, the branches are connected by (1→6)-β-linkages.

2. Role of nitric oxide in wound repair

Nitric oxide (NO) is a short-lived free radical that is involved in many important biological functions. As a testimony to the rapidly expanding knowledge about its multiple biological roles, NO, after its discovery in 1987, was named molecule of the year in 1992.[15] The NO synthases exist in three distinct isoforms, two constitutives (endothelial and neuronal) and one inducible isoform. The constitutive isoforms are permanently active generating low concentrations of NO. The expression, transcription, and function of the inducible isoform (iNOS) is induced by a variety of cytokines, growth factors and inflammatory stimuli on target cells which leads to release of high levels of NO compared to the amounts generated by the constitutive isoforms. Therefore, the regulation of iNOS takes places mainly at the gene level. The constitutives and inducible isoforms have only about 50% sequence homology.[16]

The high amounts of NO formed by the inducible isoform account for some of its detrimental effects in inflammatory situations such as sepsis .[17] iNOS is also released during wound healing, burn injury, endotoxin exposure, arthritis and inflammatory bowel diseases.

Before NO was known, Albina et al. investigated arginine metabolism in wounds and demonstrated increased citrulline formation which was imputed to an arginine deiminase-like activity.[18] Subsequently, generation of NO during wound healing was deduced by demonstrating increased urinary nitrate secretion after wounding.[19] Thereafter several studies confirmed these data and extended it to healing after burn injury.[20,21] In these models, urinary nitrate levels remained elevated until complete

healing had occurred. Later experiments confirmed that the highest NOS activity occurs during the early phases of wound healing.[22] With the development of NOS isoform specific antibodies and primers for transcriptional and translational analysis it was demonstrated that iNOS expression is highest in the early phase after acute inflammation.[23,24]

It is conceivable that the majority of NO synthesis is due to the inflammatory cells present during the early phase of healing, especially macrophages.[25] However, fibroblasts, keratinocytes and endothelial cells contribute to ongoing NO synthesis but to a lesser degree.[26,27] Therefore the overall time course of iNOS activity and NO generation during wound healing has to be viewed as a decreasing curve over time (Fig. 2).

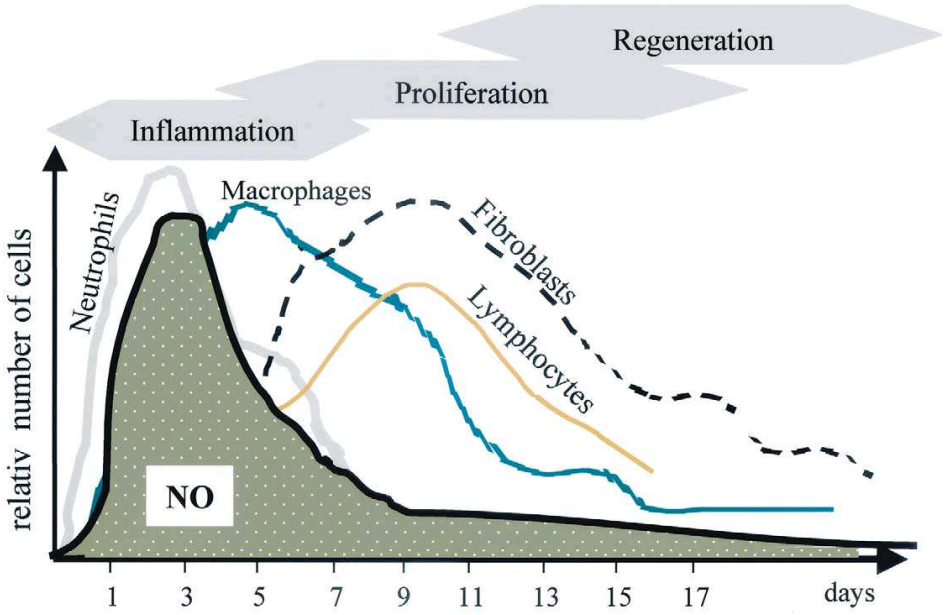

Figure 2. Phases of wound healing and the generation of wound NO.

3. Materials design for skin regeneration

Tissue engineering is emerging as an interdisciplinary field in biomedical engineering that aims to regenerate new biological material for replacing diseased or damaged tissues or organs. To achieve this, not only is a source of cells required, but also an artificial extracellular matrix (ECM) upon which the cells can be supported. Recently, some of the major advances in molecular biology have been applied to the understanding of wound healing, development and regenerative processes.[28] Tissue engineering is becoming more aware of this knowledge base and there are now moves towards designing artificial tissues and organs using both cells and specifically designed materials.

The skin, the largest organ of the body in vertebrates, is composed of the epidermis and dermis with a complex nerve and blood supply. A third layer, the hypodermis, is composed mainly of fat and a layer of loose connective tissue. These three layers play an important role in protecting the body from any mechanical damage such as wounding.

Engineering of skin substitutes implies deliberate design and fabrication according to specific functional objectives.[29] So far, that design specification in skin has relied upon the creation of both artificial dermal and epidermal components which when combined produce a replacement skin, which can be grafted in place.[30] Materials used as artificial ECM to date include those derived from naturally occurring materials and those manufactured synthetically. Examples of natural materials include polypeptides, hydroxyapatites, collagen and chitosan. Such materials have

the advantage that they have low toxicity and a low chronic inflammatory response. Examples of synthetic materials include polyglycolide, polylactide and polylactide coglycolide, which are used for sutures and meshes[31]; other examples include polytetrafluoroethylene and polyethylene terephthalate. The ultimate goal of tissue engineering of the skin is to rapidly produce a construct that offers the complete regeneration of functional skin, including all the skin appendages (hair follicles, sweat glands and sensory organs) and layers (epidermis, dermis and fatty subcutus) with rapid take (vascularization) and the establishment of a functional vascular and nerve network and scar-free integration with the surrounding host tissue (Fig. 3).

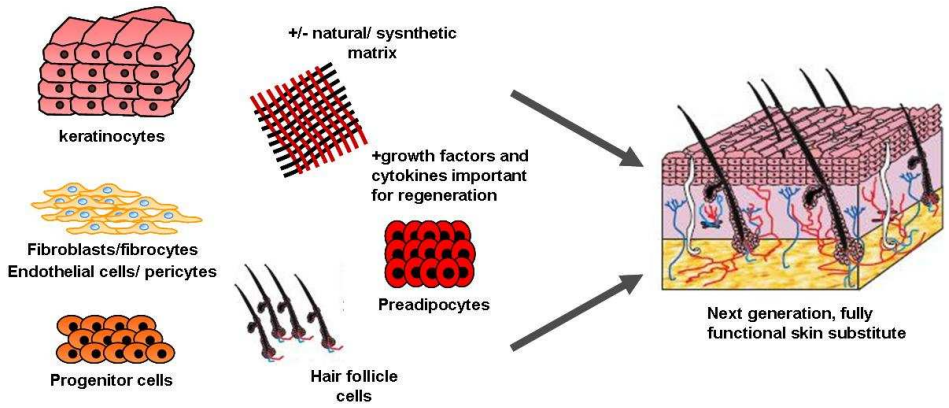

Figure 3. A schematic of the requirements to create a fully functional skin substitute.

4. Poly(lactide -co-glycolide acid)

The earliest, most successful and frequent biomedical applications of biodegradable polymers have been in tissue engineering. Examples include poly(lactic acid) (PLA), poly(glycolic acid) (PGA), poly(lactide-co-glycolide) (PLGA), poly(Ɛ-caprolactone) (PCL), polyanhydrides. The chemical structures of PLA and PGA are similar except that PLA has a methyl pendant group making it more hydrophobic, and this contributes to differences in their degradation kinetics. As a result, the degradation rate of PLGA depends on the molar ratio of lactide and glycolide resent in the polymer. An increase in lactide ratio causes gaster degradation due to decreased crystallinity. The polymer characteristics also depend on sterochemistry. The racemic poly(D,L-lactide)(DL-PLA) is less crystalline and has a lower melting point than the two steroregular polymers, D-PLA and L-PLA. The PLGA is esters of α-hydroxy acetic acid and breakdown by bulk hydrolysis of ester bonds to their constituent monomers, lactic and glycolic acid, which are eliminated from the body through Kreb's cycle(Fig 4).[32,33] Also, the degradation rate of PLGA can be controlled by varying the ratio of its co-monomers, lactic acid and glycolic acid.

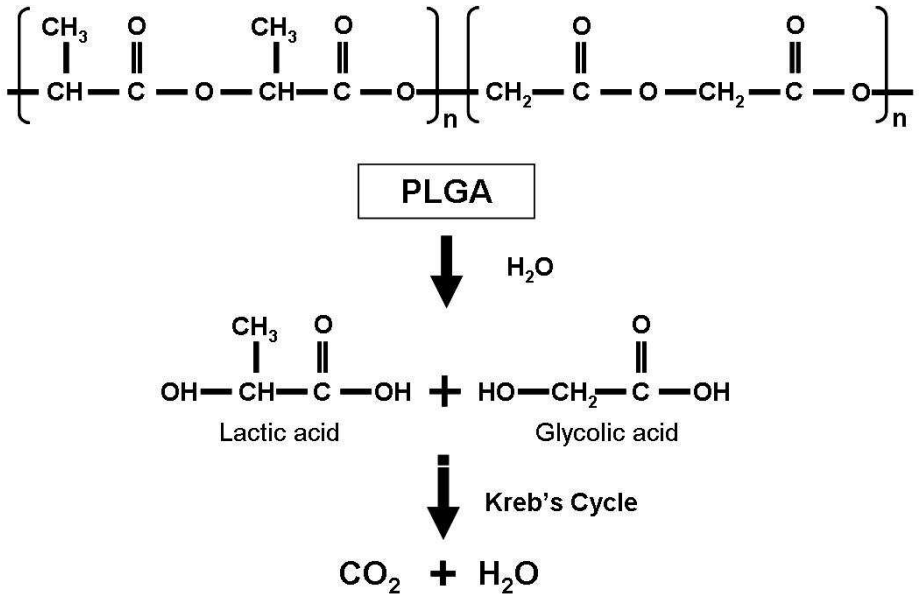

Figure 4. A schematic illustration of PLGA hydrolysis.

5. Objectives of this study

The purpose of this study is the evaluation of effects of (1→3),(1→6)-β-D-glucan (β-glucan) on wound healing *in vitro* and enhance the cellular responses of adult human dermal fibroblast (aHDFs) and Adipose tissue-derived mesenchymal stem cells (ADSCs) onto the surface-modified composite of β-glucan and PLGA by electrospinning.

In this work, we investigated whether β-glucan isolated from *Aureoubasidium* could enhance dermal wound healing. Furthermore, we studied enhance the cellular responses of aHDFs and ADSCs onto the β-glucan/PLGA composite by electrospinning and biological safety test of β-glucan/PLGA composite scaffold.

II. Materials and methods

1. (1→3),(1→6)-β-D-glucan

Water soluble (1→3)-β-D-glucan (β-glucans) that have β-D-gluccopyranosyl units attached by (1→6) linkages as single unit branch were obtained from Asahi Denka Co., Ltd. (from *Aureoubasidium pullulans*, Tokyo, Japane). β-glucan was obtained as a powder form among which about 95 % is β-glucan. The powder β-glucan was stocked as 10 mg/ml dissolved in distilled water or cell medium followed by filtering with syringe. Stocked β-glucan was colorless and odorless with low viscosity.

2. Cells

A. Cells isolations

Adipose tissue-derived mesenchymal stem cells (ADSCs) were isolated from freshly excised human subcutaneous fat tissue. After mincing into small pieces of 2-3 mm^3, adipose tissue was washed with Dulbecco's phosphate buffered saline (DPBS). Digestion of adipose tissue was performed with 0.05% collagenase typeI (Sigma Chemical Co., St Louis, MO) and 1% BSA dissolved in collagenase buffer (100mM HEPES, 120mM NaCl, 50mM KCl, 1mM $CaCl_2$, 50mM glucose, pH7.4) for 30min at 37℃ under constant shaking. The tissue slurry was filtered through a 250m filter and centrifuged at 500 x g for 20 min at room temperature. After discarding supernatant, the cell pellet was resuspended in Dulbecco's minimum essential medium supplemented with 10 % fetal

bovine serum. Cells were grown to subconfluence, trypsinized after washing, and subcultured.

B. Cells and cell cultures

Adult human dermal fibroblasts (aHDFs) were obtained from Cambrex BioScience Walkersville, Inc. The cells were cultured in Dulbecco's modified Eagle's medium (DMEM, WelGENE Inc., Daegu, South Korea) containing 10% heat-inactivated fetal bovine serum (FBS, WelGENE), 25mM HEPES (pH 7.5) and a 1% antibiotic antimycotic solution (including 10,000 units penicillin, 10 mg streptomycin and 25g amphotericin B per ml, WelGENE).

RAW264.7 cells, a mouse macrophage cell line, were obtained from American Type Culture Collection (Manassas, VA, USA). The mammalian cells were cultured in DMEM containing 10% FBS, 1% antibiotic antimycotic solution without phenolred.

The isolated ADSCs were maintained in Dulbecco's modified Eagle's medium/F12 (WelGENE), supplemented with 10% FBS (WelGENE), 10 ng/ml hEGF (CytoLab Ltd., Rehovot, Israel), 2 ng/ml hFGF (CytoLab Ltd.) and a 1% antibiotic antimycotic solution (WelGENE). All the cell maintained at 37℃ in a humidified atmosphere containing 5% CO_2. For all experiments, the cells were grown to 80–90% confluence, and subjected to no more than 15 cell passages.

3. Cell attachment assay and Cell proliferation assay

The aHDFs and ADSCs were inoculated in culture wells (24-well culture plate, Falcon, NJ, SUA) with 1㎖ growth medium containing 2×10^4 cells, respectively. The cells were treated with (1→3),(1→6)-β-D-glucan ranging from 10 to 1000 ㎛M. The cells were incubated for 4hr(for attachment assay) and 1, 3, 5day (for proliferation assay). The proliferated cells were quntified using MTT assay which measures the mitochondrial dehydrogenase activity of living cells, based on the reduction of the yellow tetrazolium salt-3-(4,5-dimethylthiazol-2-yi)-2,5-diphenyltetrazolium bromide (MTT, Sigma) by metabolically activity cells to form insoluble purple formazan crystals and was used to estimate cell viability and proliferation.[34] After cell incubation, the cells were incubated with 0.5 ㎎/㎖ MTT reagent in the last 4 h of the culture period tested at 37 ℃ in the dark. The media were decanted and then washed twice with PBS. Subsequently, the produced formazan salts were dissolved with dimethyl sulphoxid and the solution was transffered to a 96 wells plate (Falcon, NJ, USA). The absorbance was measured using an ELISA reader (Spectra Max 340, Molecular Device Inc., CA, USA) at a wavelength of 570 nm.

4. cell migration assay

This present study attempted to evaluate the effect on migration of aHDFs and ADSCs by (1→3),(1→6)-β-D-glucans. Both cells (1 x 10^5 cells/ml) were seeded in the 4-well chambered cover-glass slide (NUNC, Roskilde, Denmark) and grown to confluence overnight. Monolayers were wounded using a plastic micropipette tip and 1 mg/ml β-glucan was treated to the attached cells.[35] The cells were incubated in the CO_2 mini-incubator placed on the microscope stage for 36 hours, and visualized for migration of cells into denuded space by the charge-coupled device (CCD) camera (Electric Biomedical Co. Ltd., Osaka, Japan) attached to the inverted microscope (Olympus Optical Co. Ltd., Tokyo, Japan).

A. CO_2 mini-incubator

In order to incubate the cells on the stage of an inverted microscope, a CO_2 mini-incubator (150x130x40mm) was designed and fabricated with a double-layered acrylic plate. The mini-incubator was connected with a CO_2 incubator (MCO-15AC, Sanyo Electric Co., Ltd., Osaka, Japan) and a mini-pump to supply CO_2, and placed on the stage of an inverted microscope. The inverted microscope connected with a color CCD camera conveyed the images from the mini-incubator as a real time-mode and a frame grabber card in computer captured these images at regular intervals and memorized them as JPEG image files.

B. Image processing for single cell tracking

The captured 8-bit color images was converted into gray scale images after incorporating into the image analysis software programmed by MATLAB V7.0 (MathWork Inc., USA) and Visual Basic V6.0 language (Microsoft, USA). The edge point of each cell was detected and then the center of the detected edges was determined. The migration of the center was recorded and the time lapse and average graphs of cell movement speed was obtained. Unlike the preexisted systems, this cell tracking system has an advantage on the time lapse tracking of single cells.

5. Measurement of Nitric oxide Production

The RAW264.7 macrophages ($1x10^5$ cells/mL) were cultured in 96-well plates with 200㎕ of medium (phenol red-free RPMI 1640 medium supplemented with 10% FBS) and allowed to adhere for 2 h at 37 °C. The cells were incubated for 24 h with or without 1㎍/㎖ of lipopolysaccharide (LPS; Sigma) in the absence or presence of the test compounds. As a parameter of nitric oxide (NO) synthesis, the nitrite concentration was measured by the Griess reaction using the supernatant of the RAW264.7 macrophages as previously described.[36] Briefly, 100㎕ of the cell culture supernatant were reacted with 100㎕ of Griess reagent [1 : 1 mixture of 0.1% *N*-(1-naphtyl)ethylenediamine in H_2O and 1% sulfanilamide in 5% phosphoric acid] in a 96 well plate and the absorbance was read with a microplate reader (Molecular Devices Co., Menlo park, CA, U.S.A.) at 540 nm. Nitrite concentrations were determined by using a standard curve derived from known concentrations of $NaNO_2$ prepared in phenol red-free RPMI 1640 medium.

6. Measurement of Prostaglandin E_2

Prostaglandin E_2 (PGE_2) level in RAW264.7 macrophages supernatant was measured using commercially available kits (R&D systems, Inc., Minneapolis, MN, USA) according to the manufacruewe's protocol. The limit of PGE_2 assay was 39-5000pg/㎖.

7. Western blotting

For western blotting of inducible nitric oxide synthase (iNOS) and cyclooxygenase-2 (COX-2) expression, RAW264.7 macrophages (1×10^5cells) were incubated with LPS (1㎍/㎖) in the presence or absence of β-glucan (0.1, 0.5, 1 and 2 ㎎/㎖) for 24 h and then washed twice with ice-cold phosphate-buffered saline (PBS). The cells were lysed with ice-cold RIPA buffer [150mM NaCl, 100mM Tris-HCl (pH 8.0), 1% Triton X-100, 1% Deoxy-cholic acid, 0.1% SDS, 5mM EDTA, 10mM NaF, 5mM DTT, 1mM PMSF, 1mM sodium vandidate, 20μM leupeptin, 100μM aprotinin]. The mixture was then centrifuged at 12,000 x g for 10 min at 4℃. The protein concentration was determined by the DC Bio-Rad assay using the manufacturer's protocol (Bio-Rad Laboratories, Inc., Hercules, CA). Protein samples (20 μg of total protein) were mixed with SDS-PAGE gel loading buffer supplemented with 5% of ß-mercaptoethanol and incubated at 100°C for 5 minutes before being loaded on 12.5% polyacrylamide gels. After electrophoresis, proteins were transferred to PVDF membranes. gels were run and blotted. The membrane was probed with antibodies raised against the cyclooxygenase-2 protein (Cox-2; Santa Cruz Biotechnology, Santa Cruz, CA, USA), nitric oxide synthase2 (NOS2; Santa Cruz) and a mouse monoclonal GAPDH antibody for normalization (Chemicon International, Temecula, CA, USA) as a control for protein loading. Finally, membranes were hybridized with a secondary antibody conjugated with peroxidase (Amersham Pharmacia Biotech. Inc., Piscataway, NJ, USA) and the chemoluminescent signal was detected using the enhanced chemiluminescence system (ECL, Amersham) with high-performance chemiluminescence film (Hyperfilm ECL, Amersham).

8. Fibroblast-embedded collagen gel assay

Fibroblast-embedded collagen gel assay Fibroblast-embedded collagen gel was prepared as described elsewhere.[37] The collagen solution was prepared by mixing acid-soluble porcine type I collagen (3mg/mL), a fivefold concentration of DMEM and a buffer solution (0.05mol/L NaOH, 2.2% $NaHCO_3$, 200mmol/L HEPES) in the ratio of 7 : 2 : 1 (all reagents from Nitta Gelatin Corp., Osaka, Japan). A mixture of cell suspension in serum-free DMEM and collagen solution was divided into the wells (1.0㎖/well) of a 12-well culture plate (Costar Corp., Cambridge, MA, U.S.A.), and then gelled at 37.8℃ for 30 min (final $1.0x10^5$cells/㎖ and 2.1㎎/㎖ collagen). One millilitre of serum-free DMEM was then poured on to the gel to prevent the surface from dehydrating. After a 12h incubation, the gel was separated from each well, floated and the various reagents applied. To study the influence of wound healing synthesis on β-glucan-induced collagen gel contraction, each reagent was applied 2 h before gel floating, while β-glucan was added after gel floating. At 1, 2, 6, 24 and 48 h after gel floating, the major and minor axes of each gel sample were measured using a dial calliper (Mitutoyo Organics, Tokyo, Japan), and NIH Image J software[38] was used to quantify the areas of the collagen gels. The contraction of the gel was expressed in percentages, with the surface area of the non-contracted state serving as the norm (100%). Each value is equivalent to the mean of the triplicate measurements.

9. β-glucan/PLGA composite scaffold

A. Preparation of PLGA scaffolds

PLGA polymers (lactide/glycolic=75/25) were purchased from Lakeshore Biomaterials. The number and weight average molecular weight (M_n and M_w) of PLGA was 80kDa and 120kDa. Fiberous PLGA was made by electrospinning. The PLGA solution for electrospinning was prepared by dissolving a measured amount of PLGA in Tetrahydrofuran: N,N-Dimethylformamide (8:2) at 27 ^{o}C for 24hours. The concentration of PLGA in solution was maintained at 20%(w/v). The needle used to deliver solution was connected to 18kV and 23 gauge at a flow rate of 8.5mL/h. The stainless steel plate was used for collector and the distance from needle to collector was fixed 20cm. The thickness of the fiberous PLGA sheet was determined by a digital caliper. The average thickness of the sheet was about 0.38mm by controlling the volume of the injected solution.

B. β-Glucan grafting onto PLGA scaffolds

β-glucans were grafted onto the surface of PLGA scaffolds as previously described.[39] In brief, PLGA scaffolds were sterilized with 70% ethanol for 5 min, immersed in 2 mg/ml BG solution at 30°C for 10 min and then freeze-dried at -40°C. The resultant product was considered as a composite of β-glucans and PLGA.

.

10. Characterizations β-Glucan/PLGA composite

A. Viability and proliferation assays

Cell viability and proliferation in the β-Glucan/PLGA scaffolds were quantified by MTT assay. Approximately $5x10^4$ cells were seeded into each well of a 48-well plate with or without the β-Glucans/PLGA scaffold (0.6 cm^2) (area of the culture well: 0.8 cm^2). In order to isolate and measure the proliferation of cells inside the scaffold exclusively, the scaffolds were transferred from the original culture well to another well filled with 200mL of fresh media at each time point before measurement. Twenty microliters of MTT solution were added to the scaffold, the original culture well and the monolayer culture control, respectively. Upon addition of reagents, the cells were incubated at 37.1℃ for 1 h and the absorbance were determined at 490 nm. Cell viability and proliferation were evaluated on Day 0, 1, 5 and 10.

B. Scanning electron microscopy (SEM)

SEM (Hitachi S-800, Tokyo, Japan) was used to determine cell growth on the β-glucan/PLGA scaffolds. The scaffolds were mounted and sputter -coated with gold/platinum using an ion coater (Hitachi E-1010) and then observed at an accelerating voltage of 15kV.

11. biological safety test of β-Glucan/PLGA composite scaffold

A. Cellular toxicity Test by extract dilution method

As descried by Lee at al.[40], the MTT assay method was performed. The extracts of the β-glucan/PLGA composite scaffolds were prepared by shaking at 100rpm for 72hrs at 37℃ and serially diluted by adding fresh DMEM containing FBS (100%, 50%, 25%, 12.5%). Test System Management: L-929, mouse fibroblast cells, (ATCC CCL 1, NCTC Clone 929, of strain L) were propagated and maintained in open wells containing single strength DMEM supplemented with 10% FBS and 1% antibiotic-antimycotic solution in a gaseous environment of 5% CO_2. For this study, cells were seeded into each well of a 24-well plate in triplicate and incubated at 37°C for 24hours in order to obtain confluent monolayer's of cells prior to use. All cultures were incubated for 24h, under the same growth conditions as mentioned above. After incubation, each culture was stained with MTT solution and lysed with DMSO solution. Absorbance was measured at 570nm with an automatic microplate reader. The relative cell viability was expressed as a percentage of the optical densities in the medium containing diluted extracts to the optical densities in the fresh control medium.

B. Intracutaneous (intradermal) reactivity test

A minimum of 3 healthy adult albino rabbits (New Zealand White variety) of either sex were obtained from an approved supplier, traceable in Yonsei Medical Technology & Quality Evaluation Center records. The animals were acclimated to the laboratory for at least 3d. All animals

weighed in excess of the 2.0kg minimum ISO weight limit. The test article was extracted in 0.9% sodium chloride and cotton oil with a ratio of 6㎠/㎖ at 70°C for 24h. Each rabbit received three sequential 0.2mL intracutaneous injections on either side of the dorsal mid-line; test article extracts on one side and concurrent vehicle controls on the other. Observations for erythema and edema were carried out at 24, 48 and 72h after the injections. The irritation reactions were scored on a 0 to 4 basis. Any adverse reactions at the test sites were also noted (Table 1).

Table 1. Primary Irritation Response Categories in the Rabbit

Response Categories	Comparative Mean Score
Negligible	0 to 0.4
Slight	0.5 to 1.9
Moderate	2 to 4.9
Severe	5 to 8

C. Sensitization Test

The method described by Magnusson[41,42] as used to evaluate the allergic contact sensitization potential. A guinea pig maximization test was performed to evaluate the potential for delayed dermal contact sensitization of the test article. A minimum of 20 healthy adult albino guinea pigs of either sex were obtained from an approved supplier, traceable in Yonsei Medical Technology & Quality Evaluation Center records. The animals were acclimated to the laboratory for at least 5d. The range of animal weights at first treatment was 300g to 500g. A known sensitizing agent, 1-chloro-2,4-dinitrobenzene (DNCB) was used as the positive control. Ten test guinea pigs (per extract) were injected with the test article and Freund's complete adjuvant (FCA), and five guinea pigs were injected with the corresponding control blank and FCA (Intradermal Induction Phase). On day 6, the areas on the injection sites were treated with 10% sodium dodecyl sulfate (SDS). The day following the SDS treatment, the test animals were topically patched with the appropriate test extract and the control animals were patched with the corresponding control blank (Topical Induction Phase). The patches were removed after 48 h of exposure. Following a two week rest period, the test animals were topically patched on a previously untreated area with the appropriate test extract, while the same was done for the control animals using a control blank (Challenge Phase). The patches were removed after 24 h of exposure. The dermal patch sites were observed for erythema and edema 24 and 48 h after patch removal. Each animal

was assessed for a sensitization response based upon dermal scores (Table 2).

Table 2. Dermal Observation Scoring

Erythema (ER)	Edema (ED)
0 = No erythema	0 = No edema
1 = Slight erythema	1 = Slight edema
2 = Well defined erythema	2 = Well defined edema
3 = Moderate erythema	3 = Moderate edema
4 = Severe erythema to slight eschar formation	4 = Severe edema

12. Statistical analysis

All results were expressed as a mean±standard deviation and analyzed by Student *t*-test (Excel 2005, Microsoft, WA USA). Statistical significance was considered at $p < 0.05$.

III. Results

1. Effect of (1→3),(1→6)-β-D-glucan on cells proliferation

Figure 3, 4 show the effect of β-glucans on the cellular responses such as attachment and proliferation. There was no significant difference in the attachment of at aHDFs between the non-treated and β-glucan treated after 4h of incubation (Fig. 5A). On the other hand, the cell proliferation was significantly ($p<0.05$) enhanced on the treated β-glucan after 3d (Fig. 5B). When the cells were treated with β-glucan concentrations similar to those used in the experiments mentioned above, a significant ($p<0.05$) dose-dependent expansion (by about 60%) of cell proliferation was observed in comparison with control (Fig. 5B).

However, as shown in Fig. 6 there was no significant difference in attachment and proliferation rate between β-glucan-treated and non-treated ADSCs.

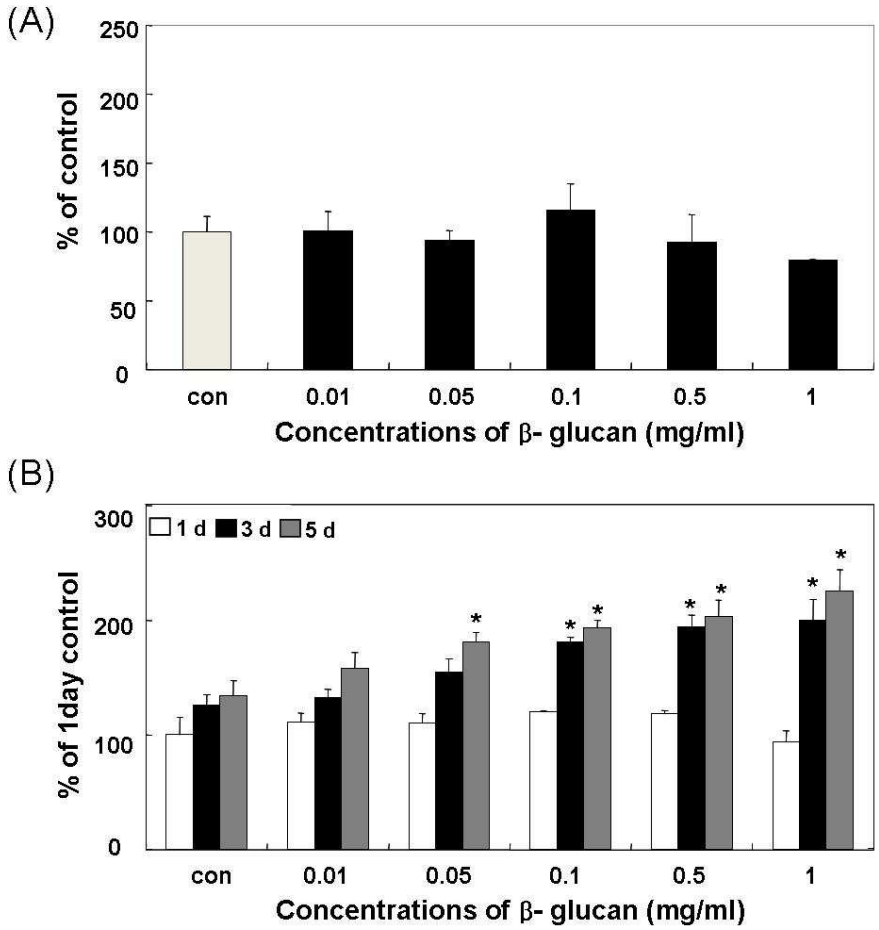

Figure 5. Effect of β-glucan on proliferation of aHDFs. The results are shown as a mean ± standard deviation (n = 3). (A) attachment of aHDFs. (B) proliferation of aHDFs. The data is analyzed by Student t-tests, and the values are significantly ($p< 0.05$) different from the non-treated control. The cell proliferation was significantly enhanced on the treated β-glucan after 5d.

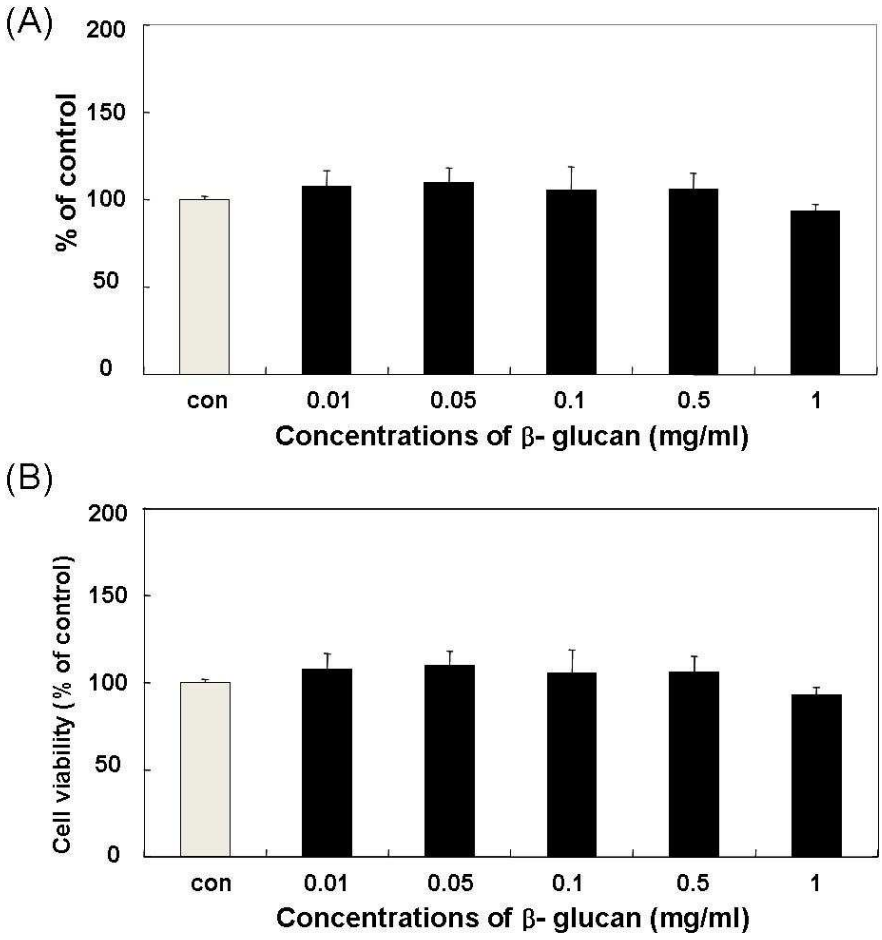

Figure 6. Effect of β-glucan on proliferation of ADSCs. The results are shown as a mean ± standard deviation (n = 3). (A) attachment of ADSCs. (B) proliferation of ADSCs. The data is analyzed by Student t-tests, and the values are significantly ($p< 0.05$) different from the non-treated control. There was no significant difference between β-glucan-treated and non-treated groups.

2. Effect of (1→3),(1→6)-β-D-glucan on migration

Cell movement is a combined effect of cell division and cell migration .[43] The migratory function of cells could be isolated by subjecting them to pre-treatment with Mitomycin C, an agent capable of inhibiting cell division but not cell mobility.[41,44,45] To examine whether β-glucan exhibited biological effects relevant to migration of aHDFs and ADSCs, wound healing migration assay were performed (Fig 7, 8). The speed of β-glucan treated group remained faster than non-treat group. Furthermore, the average migration speed of the 1 ㎎/㎖ β-glucan treated aHDF was 67.1 ㎛/hr, while that of the non-treated group was 45.5 ㎛/hr (Fig 7). On the other hand, the cell proliferation assay of ADSCs showed that there was no increasing effect of β-glucan on the proliferation. However, the cell migration assay showed that β-glucan have effect on the migration of ADSCs. The average migration speed of the 1 ㎎/㎖ β-glucan treated ADSCs was 86.3 ㎛/hr, while that of the non-treated group was 72.1 ㎛/hr (Fig 8).

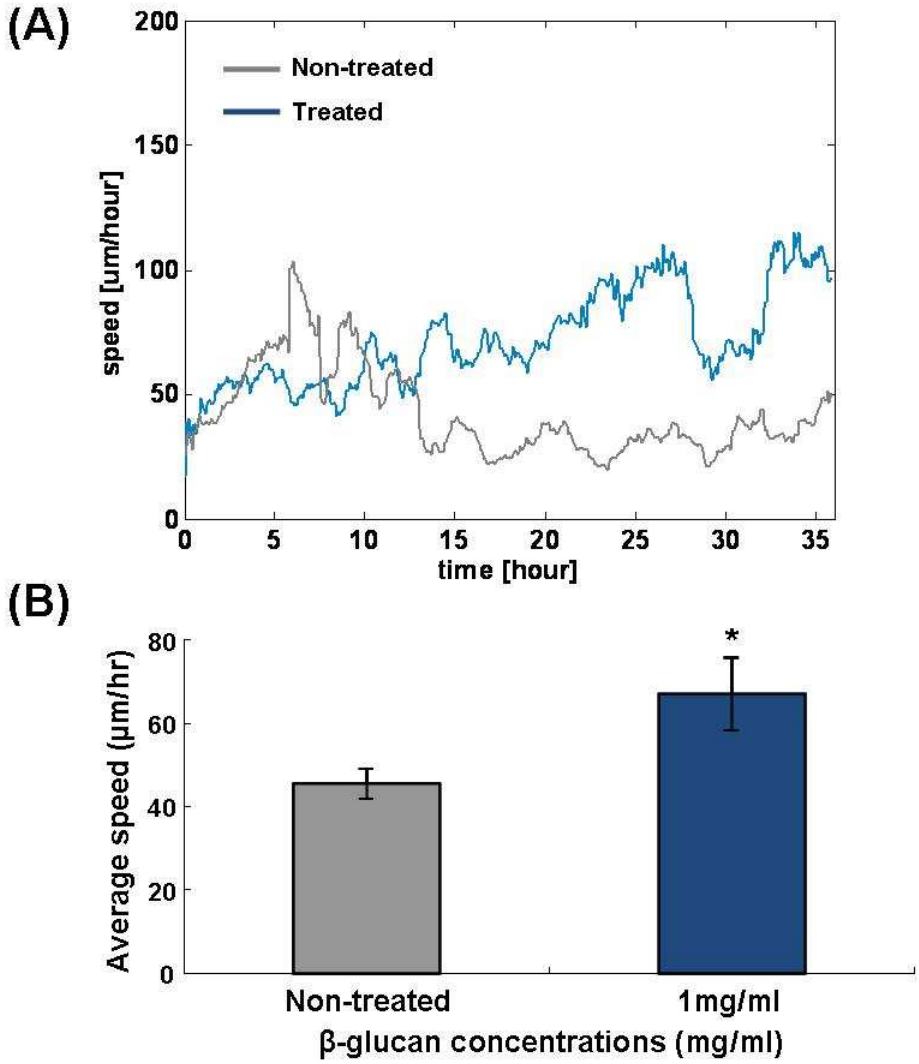

Figure 7. Effect of β-glucan on migtration of aHDFs. (A) Real time migration speed of β-glucan treated and non-treated aHDFs. (B) Average migration speed of β-glucan treated and non-treated aHDFs. β-glucan treated cells were migrated faster than control. Data are expressed as mean ± standard deviation (n=3). Analyzed by t-tests and statistical significance was considered as $p< 0.1$.

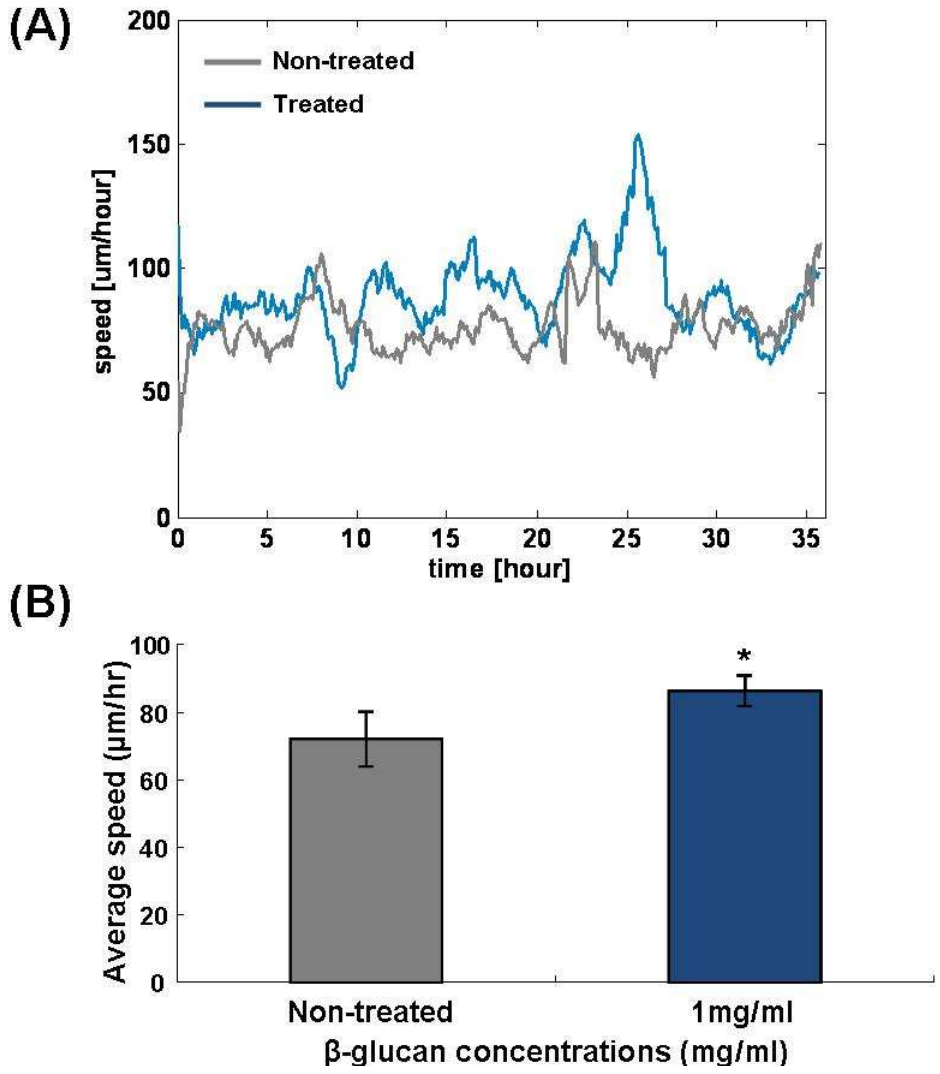

Figure 8. Effect of β-glucan on migtration of ADSCs. (A) Real time migration speed of β-glucan treated and non-treated ADSCs. (B) Average migration speed of β-glucan treated and non-treated ADSCs. β-glucan treated cells were migrated faster than control. Data are expressed as mean ± standard deviation (n=3). Analyzed by t-tests and statistical significance was considered as $p< 0.1$.

3. Measurement of NO Production

NO is synthesized from L-arginine by NOS. For the expression of iNOS, the mammalian cells should be triggered by specific stimulants, such as pro-inflammatory cytokines and bacterial LPS.[46] Since iNOS-derived NO is involved in various pathological conditions such as inflammation and autoimmune diseases and leads to cellular injury,[47] suppression of iNOS is closely linked with anti-inflammatory action. Inhibitory effect of β-glucan was assessed on LPS-induced NO production in RAW264.7 macrophages (Fig. 9). The accumulated nitrite, determined by the Griess method, in the medium was used as an index for NO level. After treatment with LPS, nitrite content notably increased. When the RAW264.7 macrophages were treated with 0.5, 1.0 and 2.0 mg/ml β -glucan, NO production induced by LPS was significantly inhibited in a dose-dependent manner (Fig. 9).

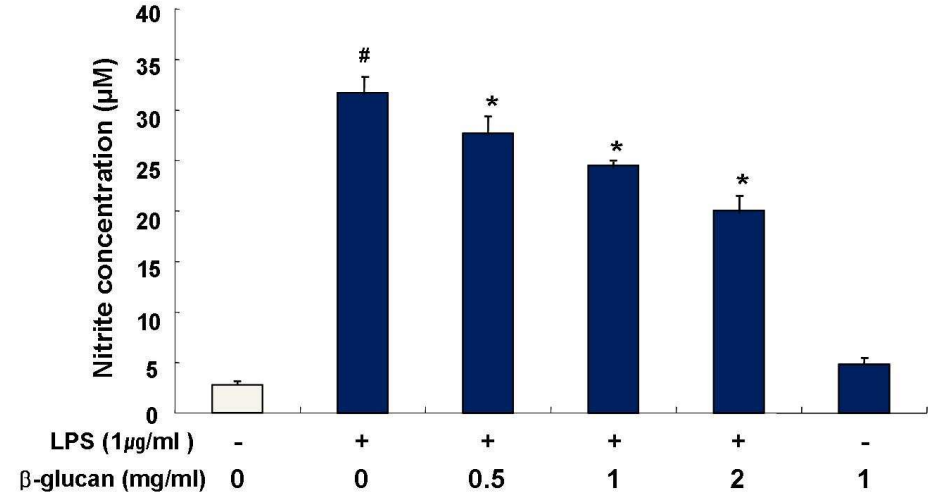

Figure 9. Inhibitory effect of β-glucan on LPS-induced NO production in RAW264.7 macrophages. The RAW264.7 macrophages were incubated for 24 h with LPS (1㎍/㎖) in the presence or absence of indicated concentrations of β-glucan. Accumulated nitrite in the culture medium was determined by the Griess reaction. The values are mean ± S.E. of the three independent experiments. # $P < 0.05$ compared to control; * $P < 0.05$ compared to LPS.

4. The effects of β-glucan plus LPS on iNOS/COX-2 protein production

In this study we demonstrated synergistic induction of the iNOS/COX-2 protein expression by the combination of the LPS, with β-glucan in RAW 264.7 macrophages (Fig. 10, 11). With the assumption that the inhibition of NO production by β-glucans would be caused by a decrease in the iNOS protein level, the effect of β-glucans on the iNOS expression was examined in the macrophages cells treated with LPS. As shown in Fig. 7, β-glucan dose-dependently suppressed iNOS induction without changes in the levels of GAPDH, an internal control, indicating the specific inhibition of iNOS expression by β-glucan. Suppressive effect of β-glucan on the production of NO was confirmed *in vivo* experiments.

The strong reduction in the exudate by β-glucan might attribute to the presence of antioxidant compounds in β-glucan. β-glucan also appeared to suppress induction of COX-2 in LPS-stimulated RAW264.7 macrophages (Fig. 11). When β-glucans were added together with LPS (1㎎/㎖ for iNOS assay), the levels of the iNOS and COX-2 protein expression was decreased about 2.8 and 5.8-fold than the addition of any inducer alone (Fig. 10 and Fig. 11). It is likely that β-glucan shows its anti-inflammatory activity through the down-regulation of NO production and COX-2 in the inflammatory process. The densitometric analyses were plotted by image analysis software (ImageJ, National Institutes of Health, USA).

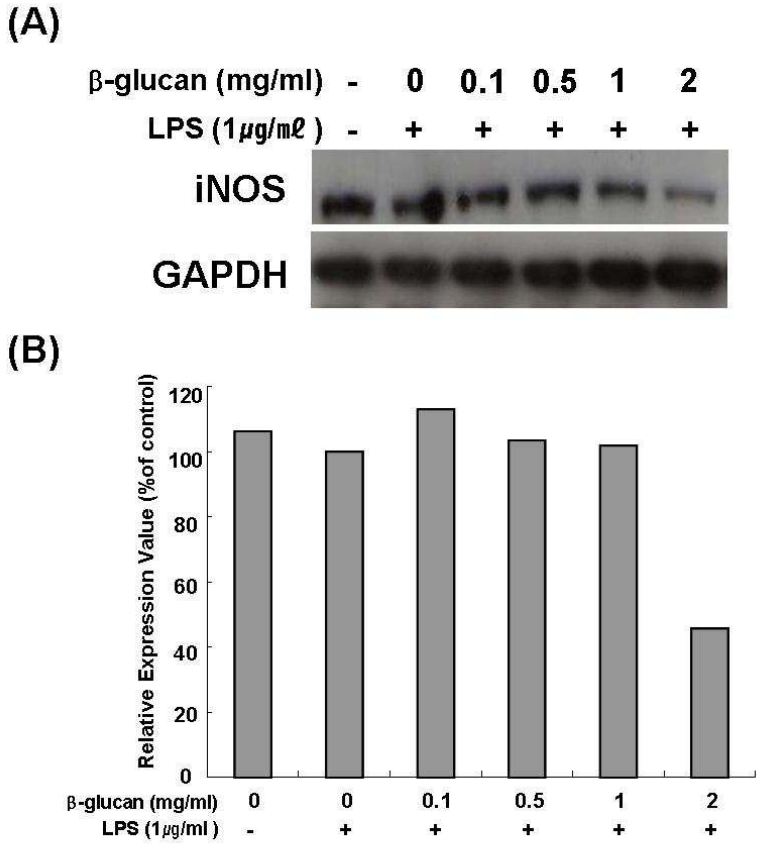

Figure 10. The effect of β-glucan on expression of inducible nitric oxide protein production (A) and densitometric analyses of western blot (B). After densitometric analysis, data were expressed as a percentage of values for stimulated cells with LPS (1㎍/㎖). Data represent of 3 independent experiments.

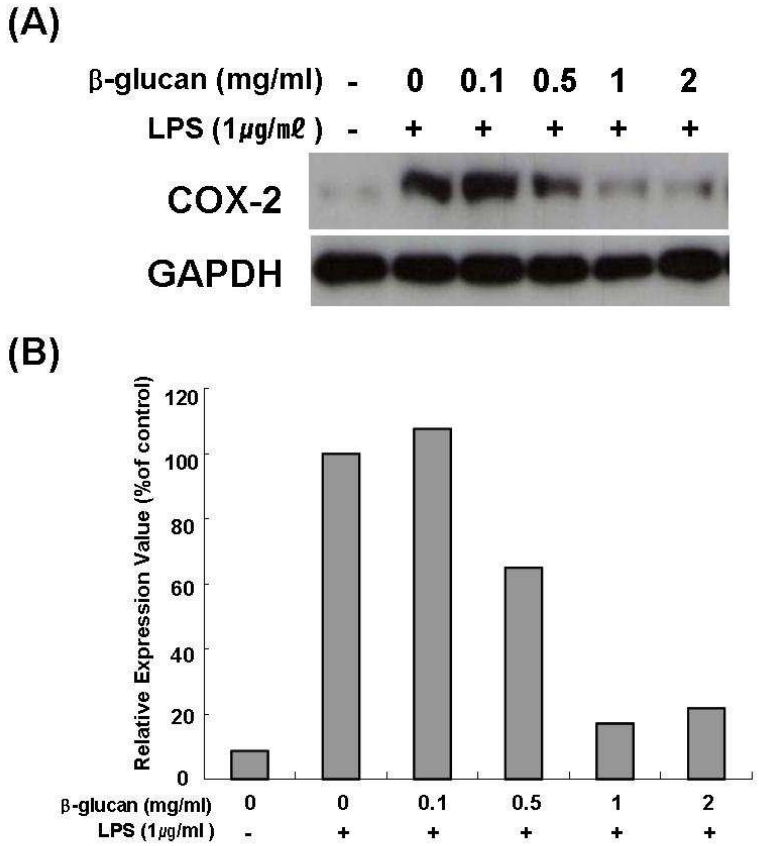

Figure 11. The effect of β-glucan on expression of cyclooxygenase-2 protein production (A) and densitometric analyses of western blot (B). After densitometric analysis, data were expressed as a percentage of values for stimulated cells with LPS (1㎍/㎖). Data represent of 3 independent experiments.

5. PGE_2 release from β-glucan-stimulated macrophages in a COX-2 dependent way

To investigate the role of β-glucan-induced COX-2 expression on the PGE_2 production, RAW264.7 macrophages, first, were inoculated with β-glucans between 0.1 and 2㎎/㎖ for 8 h, and PGE_2 expression was measured using ELISA assay. Result demonstrated that PGE_2 release from RAW264.7 macrophages was significantly increased by LPS(1㎍/㎖) (Fig. 12). Furthermore, the pre-treatment of selective COX-2 inhibitor β-glucan significantly decreased LPS-induced PGE_2 production to baseline levels in RAW264.7 cmacrophages. Taken together, these data indicate that LPS-induced PGE_2 production was mediated by COX-2 dependent pathway, but independently from COX-1 pathway.

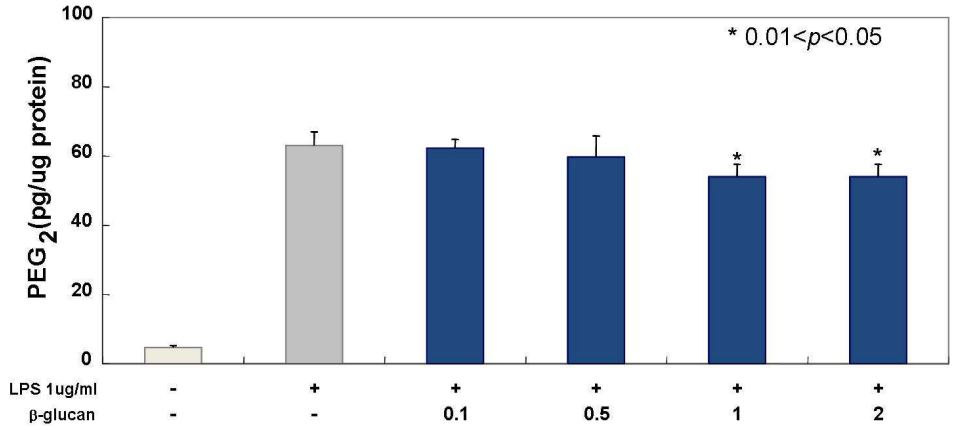

Figure 12. Effects of β-glucan on PGE_2 accumulation in LPS-stimulated RAW 264.7 macrophages. After RAW 264.7 macrophages were treated with LPS (1㎍/㎖) and various concentrations of β-glucan for 8hrs. PGE_2 accumulation was determined as described in Methods section. Data represent means ± SEM of 3 independent experiments.

6. Collagen gel contraction assay

Three-dimensional collagen gels have been used as in vitro systems for modeling of cellular activities during wound healing.[48] This model system was adapted to assess the capability of β-glucan to induce collagen gel contraction in concert with cellular activities. These results were depicted in Fig. 10. Collagen gels with β-glucan contracted strongly after 4 h of incubation post-gelation; whereas, there was no obvious change in gel size in the non-treated control (Fig. 13(A)). The magnitudes of gel contraction were summarized in Fig. 13(B). After 24 h of incubation, the presence of cell treated β-glucan (1㎎/㎖) rendered the collagen gel to contract to approximately 41.1% of its original size. In contrast, cell-laden collagen gel (without β-glucan) contracted to 72%. For comparison, the gel contracted to 74.8% ($p<0.05$) of its original size in the absence of cells ($p<0.05$).

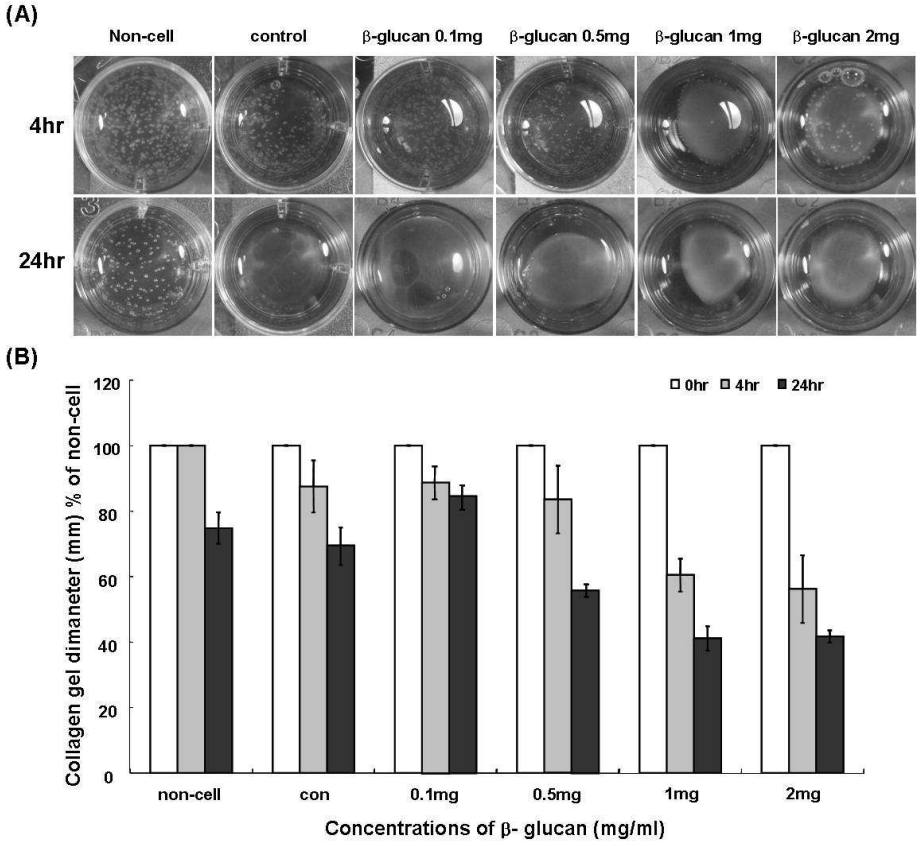

Figure 13. Collagen gel contraction assay: (A) Collagen gel contractions were monitored at 0, 4 and 24 h after gelation. (B) Area changes of the collagen gels at 4 and 24 h after gelation.

7. Proliferation of cells onto PLGA scaffold and β-glucan/PLGA composite scaffold

To further analyze the ability of a scaffold to influence the growth of cultured cells, aHDFs and ADSCs were cultured in β-glucan/PLGA scaffolds for 2 weeks and cell ability was assayed with MTT methods at various points along this time course (see in Fig. 14, 15). PLGA scaffolds were used as controls. The cell density of the β-glucan/PLGA scaffold was significantly higher than that of the PLGA scaffold. The 3D and high porosity structure of the β-glucan/PLGA scaffold and thus, availability of void volume enabled the continual proliferation of cells and this accounted for the significantly higher optical density observed.

8. Morphological and structural characteristics of β-glucan/PLGA composite scaffold

This finding was in good agreement with the scaffold histology results presented above (see Fig. 16(A) and (B)). The cells residing in the scaffold continued to proliferate reaching by day 10. It was known that strong cell adhesion and spreading on biomaterial facilitates cell proliferation.[49]

Figure 16(A) and (B) show the SEM images of aHDFs on PLGA scaffold and β-glucan/PLGA composite scaffold. aHDF cultured on the PLGA scaffolds were rounded in shape instead of a spreading morphology, whereas on the β-glucan/PLGA composite scaffold aHDFs adopted a spreading polygonal shape which is typical of the normal cell

morphology on Tissue culture plates (TCP_S). These characteristics are prerequisites for an effective re-epithelialization of artificial skin materials.

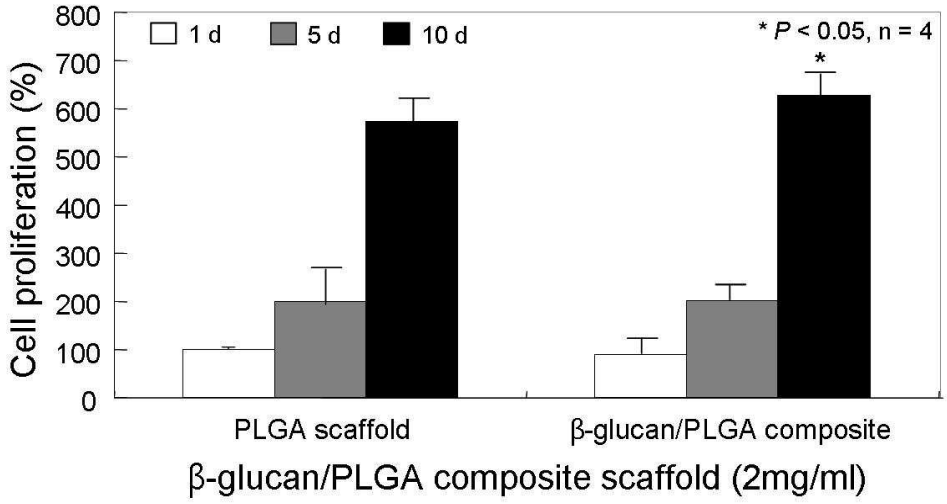

Figure 14. Proliferation of aHDFs onto non-treated and β-glucan/PLGA composite scaffold (* $p<0.05$ vs. the non-treated at the same time, analyzed by a Student's *t*-test, n=4).

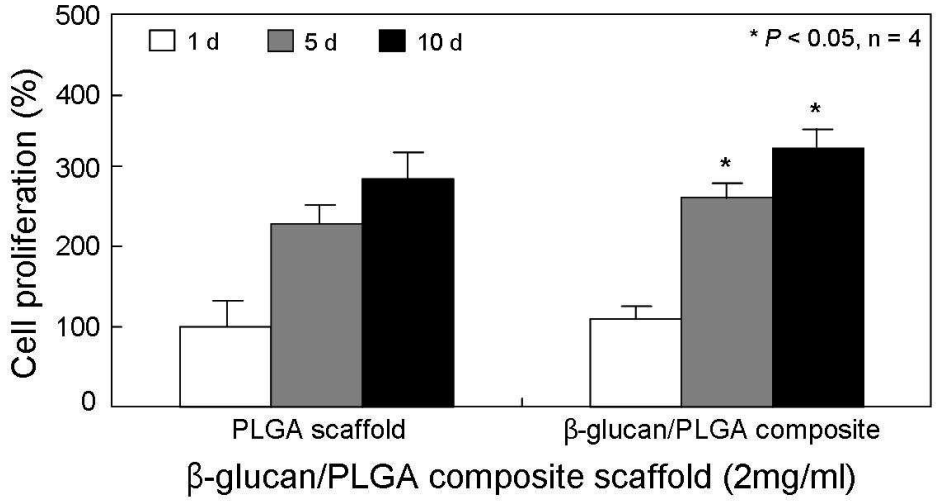

Figure 15. Proliferation of ADSCs onto non-treated and β-glucan/PLGA composite scaffold (* $p<0.05$ vs. the non-treated at the same time, analyzed by a Student's *t*-test, n=4).

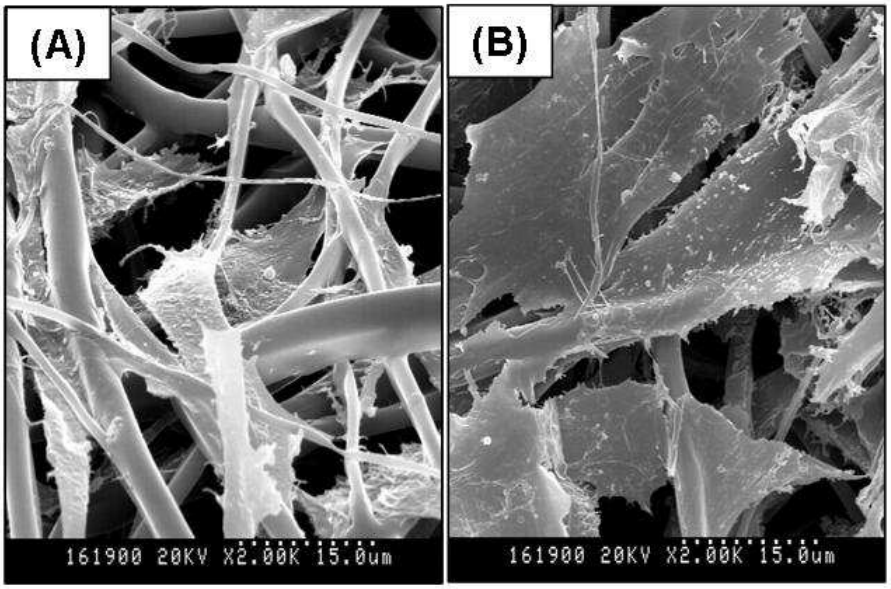

Figure 16. SEM micrographs of aHDF cultured onto either PLGA scaffold (A) or β-Glucan/PLGA composite (B). aHDFs were seeded at a density of $1x10^4$ cells and fixed for SEM study 10days later.

9. Biological safety test of β-Glucan/PLGA composite scaffold

A. Cytotoxicity Test

Using an extract dilution method, experiments for cytotoxicity was also performed in vitro for test groups as used in the above test. The characteristics of the fibroblastic cells cultured in the presence of the extracts from the 3 test materials are illustrated in Fig. 17. The number of viable cells among the fibroblasts cultured in each diluted extracts was measured. Under the conditions of this study, the test article extract showed 91.3% of cell viability compared with negative control. As anticipated, the negative control was nontoxic and the positive control was toxic (Fig. 17).

B. Intracutaneous (intradermal) reactivity test

Extracts of β-glucan/PLGA composite scaffold and negative control solutions did not trigger irritation responses at any circumstance during the skin sensitization assay. Therefore, the overall irritation response was equivalent to zero (0) for both the β-glucan/PLGA composite scaffold and solvent-exposed animals (Table 1). Based on the above results, the β -glucan/PLGA composite scaffold extracts were found to be non-sensitizing under the conditions of this experiment. No intracutaneous irritation was induced either by β-glucan/PLGA composite scaffold extracted in the saline solution. In the case of cottonseed oil extraction,

both the extracts of β-glucan/PLGA composite scaffold and the blank solution obtained a negligible to slight irritation response (PIS, Table 3). Nevertheless, the difference between extracts and blank solutions PIS was 1.0 or less in both extraction media. Based on these results, the extracts of β-glucan/PLGA composite scaffold in both saline and cottonseed oil solutions have met the requirements of the test criteria for biological responses in the intracutaneous reactivity assay. No toxic symptoms or abnormal behavior such as convulsion, prostration or sign of biological reactivity were observed with any of the mice injected with extracts or blank controls. Animals from all groups gained normal body weight and appeared healthy at all times during the 72hrs recovery period. Based on these results, the extracts in both saline and cottonseed (Fig. 18, Table 3).

C. Sensitization Test

Table 4 shows the concentrations of the test materials used in the maximization test and the skin responses following the challenge. Under the conditions of this study, the test article extract showed no significant evidence of causing delayed dermal contact sensitization (Fig. 19, Table 4).

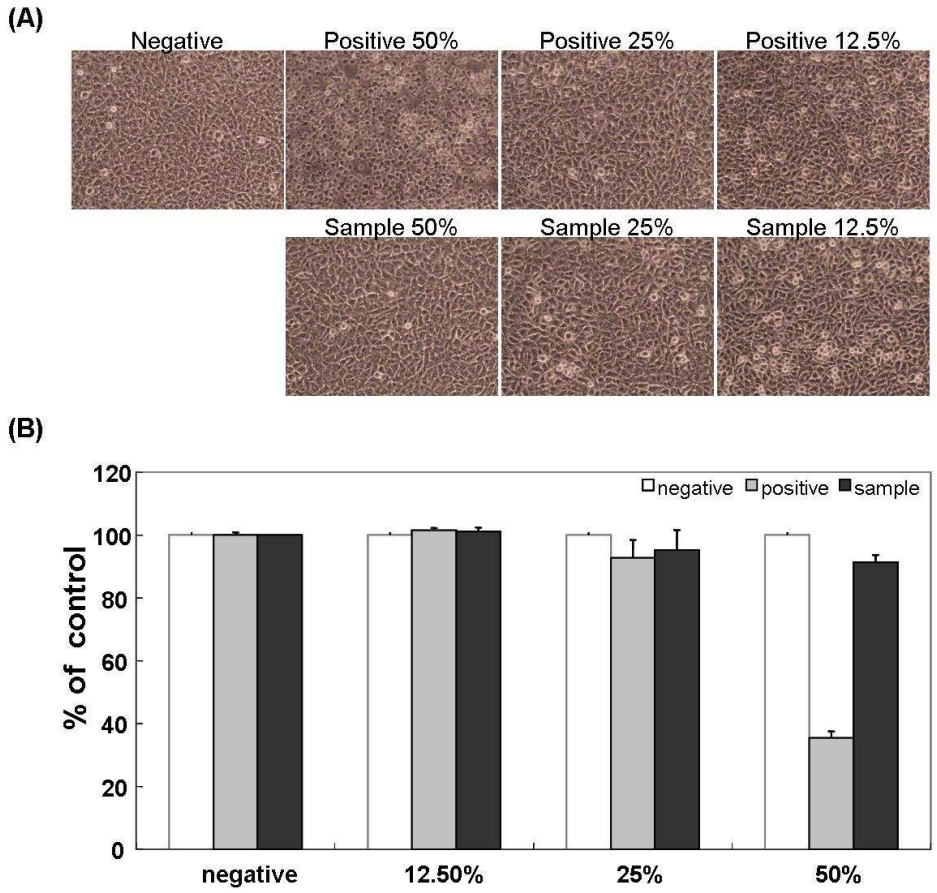

Figure 17. Cytotoxicity test of β-glucan/PLGA composite scaffold. Relative cell viability of positive control, negative control and test article extracts. (A) L-929 cells were monitored (B) densitometric analyses of MTT assay.

Figure 18. Intracutaneous reactivity test of β-glucan/PLGA composite scaffold.

Table 3. Test totals and calculation of the primary irritation score (PIS) for rabbit.

Rabbit	24 h	48 h	72 h	Sum of Observation	Observation Average
Total Test Scores	0	0	0	0	0/24
Total Control Scores	0	0	0	0	0/24

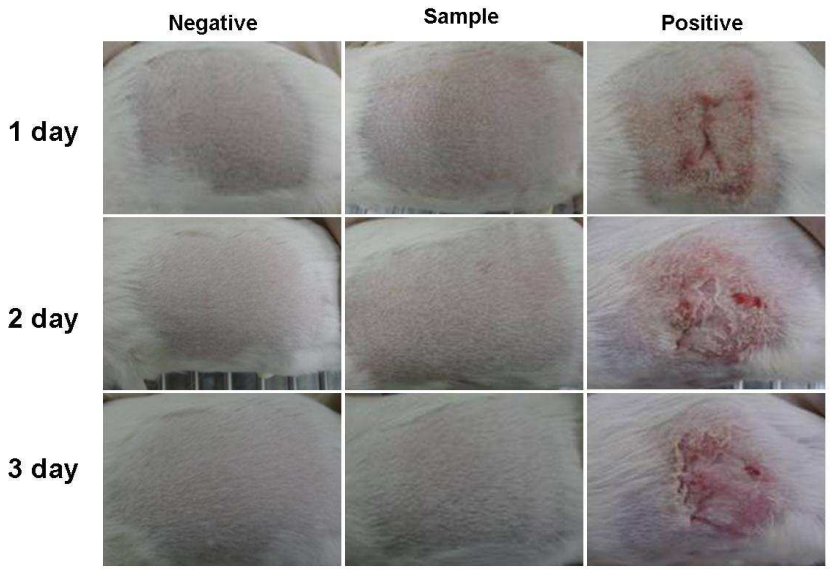

Figure 19. Sensitization test of β-glucan/PLGA composite scaffold.

Table 4. Positive control, negative control and test article extract daily challenge observations.

Experimental Group	24 h		48 h		Result
	ER	ED	ER	ED	
Positive Control	1	0	2	1	Positive
Negative Control	0	0	0	0	Negative
Test Article	0	0	0	0	Negative

IV. Discussion

In order to evaluate the effect of (1→3),(1→6)-β-D-glucan on wound healing. The cell proliferation and migration assay were conducted using aHDFs and ADSCs. β-glucan were tested for the ability as an anti-inflammatory using LPS-stimulated macrophage cell line (RAW 264.7 macrophages). Finally, we examined the effects of β-glucan/PLGA composite scaffold on cell attachment and proliferation and Biological safety of these scaffolds was evaluated.

In contact co-culture experiment, there was no difference in the attachment on both aHDFs and ADSCs 4 h after seeding. On the other hand, the cell proliferation was significantly (p<0.05) enhanced on the β-glucan after 3d. aHDFs proliferation might not be affected by the efficiency of initial attachment to the underlying lawns. In the cell migration assay, β-glucan treated group covered faster with cells than that of non-treated control. Compromised cell migration and proliferation are two of the major contributory factors for impaired healing of chronic wounds .[50-52] The migration assay results indicated that cells with impaired proliferation capacity were able to migrate along the β-D-glucan and it could be beneficial to healing of chronic dermal wound.

β-glucan inhibited LPS-stimulated iNOS induction in a concentration-mannaer. Expecially, higher concentrations (>0.5㎎/㎖) of β-glucan almost blocked iNOS induction. In addition, LPS-stimulated expression of COX-2 was inhibited by β-glucan treatment. β-glucans up to 0.5㎎/㎖ still required to inhibit COX-2 induced by LPS. Consistent with these findings, treatment with β-glucan suppressed *de novo* synthesis and cellular accumulation of PGE_2 to a lesser extent, suggesting that β

-glucan blocked the induction as well as the activity of COX-2.

Prompting the wound healing process and identifying factors affecting wound healing after β-glucan exposure is complicated, and thus it is challenging to develop new therapeutic strategies to improve the cure rate. Re-epithelialization carried out by fibroblast migration and proliferation is an important event in skin wound healing. This event is orchestrated by various growth factors produced by fibroblasts and other cutaneous cell types, including platelets, inflammatory cells, keratinocytes, and epithelial cells.[53] Recent evidence clearly indicates that NO produced by iNOS followed by NO-mediated signaling in the skin plays a pivotal role in skin wound healing.[54] However, the roles of NO in skin wound healing vary depending on the study models employed and/or the stages of the wound healing. For example, suppression or deletion of iNOS, the major producer of NO in the skin, yields delayed or no wound healing,[55] but introduction of the iNOS gene to a wounded area rescues the delayed wound healing in a mouse model.[56]

Healing fibroblasts are phenotypically characterized by changes in collagen production, cell proliferation, and migration. Wound cells have been shown to increase the expression of iNOS and production of NO in various models.[57,58] Inhibition of iNOS delayed the re-epithelialization in cutaneous wound repair.[56] The delayed wound repair in iNOS knockout mice was reversed by iNOS gene transfer.[59] Interestingly, the role of nitric oxide on cell proliferation after wounding is concentration-dependent.[60] At low concentration, NO promoted cell proliferation in murine fibroblast,[61] while at higher concentrations, NO decreased the proliferation of rat dermal skin fibroblasts.[60]

The contraction of collagen gels by fibroblasts was first reported by Bell et al.[62] and is a phenomenon useful in the study of cell to collagen

interactions (collagen morphogenesis).[63,64] We performed several experiments to study the mechanism of fibroblast mediated collagen gel contraction, focusing on the relationship among the cell surface of fibroblasts, collagen, and β-glucan. On the this study, we present an indirect interaction between fibroblasts and collagen in the process of gel contraction via β-glucan synthesized and secreted by fibroblasts. Dermal fibroblasts play key roles in skin extracellular protein turnover, ECM interaction, cell-cell communication, etc.,[50] which are closely related functions. Collectively, these data suggest that β-glucans are constitutionally well suited for dermal wound healing via.

The density of isolated β-glucans/PLGA composite scaffold was significantly higher than that of the PLGA scaffold. The results of MTT assay indicated that the β-glucan/PLGA composite scaffolds were non-toxic to cells, therefore suggested good biocompatibility despite chemical modification of β-glucan; the large pore size and the high surface area to volume ratio, and the strong binding of the cells to the scaffold indeed favored cell growth and proliferation. Compromised cell migration and proliferation are two of the major contributory factors for impaired healing of chronic wounds.[50,51]

The cell morphology, proliferation and distribution assay showed that dermal fibroblasts attached and moved to the interior of β-glucan/PLGA scaffolds without the need of incorporating any cell adhesion facilitating component. It was distinctively different from the results of other studies describing various scaffolds in which cells failed to distribute uniformly in the matrices in conjunction with the majority of them attached only to the outer surfaces.[65] Evidently, the homogeneous distribution of the multi-layered cells inside the highly porous β-glucan/PLGA scaffold resembles the structures of dermal tissue, which is a desirable feature for

dermal tissue engineering scaffold design. Lastly, the β-glucan/PLGA scaffold could also double as a carrier of cultured cells (stem cell, Xenogenic cell of animal origins) and/or bioactive agents like drugs, genes or proteins for sustained and localized delivery to the site of interest to accelerate wound closure.

V. Conclusion

In this study, we investigated the interaction between β-glucan and aHDFs/ADSCs for the first time, as the application of β-glucan for dermal wound healing remained speculative. Cell proliferation and migration assay showed that β-glucan have effect on the migration not the proliferation of ADSCs. However, β-glucan have effects on aHDFs by activating proliferation and migration activity of aHDFs. In addition, LPS-stimulated expression of COX-2 was inhibited by β-glucan treatment. Consistent with these findings, treatment with β-glucan suppressed cellular accumulation of PGE_2 to a lesser extent, suggesting that β-glucan blocked the induction as well as the activity of COX-2. Furthermore, collagen gels with β -glucan contracted strongly after 4 h of incubation post-gelation. β -glucan/PLGA composite scaffolds were shown to maintain the open porous structure with the pore interconnectivity, porosity as well as to enhance the surface roughness. Furthermore, this β-glucan treatment provided cytocompatible environments for the attachment and proliferation of both cells. These results suggest that the surface modification of a composite of a biodegradable polymer and bioactive molecule by β-glucan can enhance the cellular responses of cells and the β-glucan-treated composite may play an effective role in regenerating soft tissue with aHDFs/ADSCs.

In conclusion, our results suggested that the β-glucan/PLGA composite scaffolds are constitutionally well suited for artificial skin.

References

1. Ruiz-Herrera J. Biosynthesis of beta-glucans in fungi. Antonie Van Leeuwenhoek 1991;60:72-81.
2. Williams D, Mueller A, Browder W. Prevention and clinical evaluation of carbohydrate immunopharmaceuticals in the prevention of sepsis and septicsequelae. J End otox in Res 1995;2:203-8.
3. Williams DL, Pretus HA, McNamee RB, Jones EL, Ensley HE, Browder IW, et al. Development, phy sicochemical characterization and preclinical efficacy evaluation of a water soluble glucan sulfate derived from *Saccharomyces cerevisiae*. Immunopharmacology 1991;22:139-55.
4. Browder W, Williams D, Pretus H, Olivero G, Enrichens F, Mao P, et al. Beneficial effect of enhanced macrophage function in the trauma patient. Ann Surg 1990;211:612-3.
5. Williams D, Browder W. Development of natural product (1→3)-β-D -glucan polymers as immune stimulating pharmaceuticals. Polymer Adv Tech 1994;5:529-34.
6. Browder W, Williams D, Lucore P, Pretus H, Jones E, McNamee R. Effect of enhanced macrophage function on early wound healing. Surgery 1988;104:224-30.
7. Portera CA, Love EJ, Memore L, Zhang L, Muller A, Browder W, et al. Effect of macrophage stimulation on collagen biosynthesis in the healing wound. Am Surg 1997;63:125-31.
8. Wolk M, Danon D. Promotion of wound healing by yeast glucan evaluated in single animals. Med Biol 1985;63:73-80.

9. Delatte SJ, Evans J, Hebra A, Adamson W, Othersen HB, Tagge EP. Effectiveness of beta-glucan collagen for treatment of partial-thickness burn in children. J Pediatr Surg 2001;36:113-8.
10. Compton R, Williams D, Browder W. The beneficial effect of enhanced macrophage function on early wound healing. Am Surgeon 1996;62:14-18.
11. Wolk M, Danon D. Promotion of wound healing by yeast glucan evaluated on single animals. Lab Anim Sci 1985;35:150-2.
12. Kernodle DS, Gates H, Kaiser AB, Prophylactic anti-infective activity of poly-[1-6]-beta-D-glucopyranosyl-[1-3]-beta-D-glucopyranose glucan in a guinea pig model of staphylococcal wound infection. Antimicrob Agents Chemother 1998;42:545-9.
13. Kaiser AB, Kernodle DS. Synergism between poly-(1-6)-beta-D-glucopyranosyl- [1-3]-beta-D-glucopyranose glucan and cefazolin in prophylaxis of staphylococcal wound infection. Antimicrob Agents Chemother 1998;42:2449-51.
14. Assoian RK, Komoriya A, Meyers CA, Miller DM, Sporn MB. Tranforming growth factor-beta in human platelets. J Biol Chem 1983;258:7155-60.
15. Koshland DE. Molecule of the year. Science 1993;262:1953.
16. Knowles RG and Moncada S. Nitric oxide synthases in mammals. Biochem J 1994;298:249-58.
17. Tsukahara Y, Morisaki T, Horita Y, Torisu M, Tanaka M. Expression of inducible nitric oxide synthase in circulating neutrophils of the systemic inflammatory response syndrome and septic patients. World J Surg 1998;22:771-7.
18. Albina JE, Mills CD, Barbul A, Thirkill CE, Henry Jr WL, Mastrofrancesco B, et al. Arginine metabolism in wounds. Am J

Physiol 1988;254:459-67.

19. Smith DJ, Dunphy MJ, Strang LN, Marletta MA. The influence of wound healing on urinary nitrate levels in rats. Wounds 1991;3:50-8.
20. Becker WK, Shippee RL, McManus AT, ET AL. Kinetics of nitrogen oxide production following experimental thermal injury in rats. J Trauma 1993;34:855-62.
21. Carter EA, Derojas WT, Tamir S, Tannenbaum SR, Yu YM, Tompkins RG. Nitric oxide production is intensely and persistently increased in tissue by thermal injury. Biochem J 1994;304:201-4
22. Albina JE, Mills CD, Henry WL, Jr., Caldwell MD. Temporal expression of different pathways of L-arginine metabolism in healing wounds. J Immunol 1990;144:3877-80.
23. Frank S, Madlener M, Pfeilschifter J, Werner S. Induction of inducible nitric oxide synthase and its corresponding tetrahydrobiopterin -cofactor-synthesizing enzyme GTP-cyclohydrolase I during cutaneous wound repair. J Invest Dermatol 1998;111:1058-64.
24. Nill MR, Oberyszyn TM, Ross MS, Oberyszyn AS, Ruberg RL, Robertson FM. Quantification of inducible nitric oxide gene expression during incisional wound healing. Surg Forum XLVI 1995;46:753-5.
25. Reichner JS, Meszaros AJ, Louis CA, Henry WL Jr, Mastrofrancesco B, Martin BA, et al. Molecular and metabolic evidence for the restricted expression of inducible nitric oxide synthase in healing wounds. Am J Pathol 1999;154:1097-104.

26. Schaffer MR, Efron PA, Thornton FJ, Klingel K, Gross SS, Barbul A. Nitric oxide, an autocrine regulator of wound fibroblast synthetic function. J Immunol 1997;158:2375-81.
27. Paulsen SM, Wurster SH, Nanney LB. Expression of inducible nitric oxide synthase in human burn wounds. Wound Repair Regen 1998;6: 142-8.
28. Harty M, Neff AW, King MW & Mescher AL. Regeneration or scarring: an immunologic perspective. Dev. Dyn. 2003; 226: 268-79.
29. Boyce ST, Warden GD. Principles and practices for treatment of cutaneous wounds with cultured skin substitutes. Am J Surg 2002;183:445-56.
30. Supp DM, Boyce ST. Engineered skin substitutes: practices and potentials. Clin Dermatol 2005;23:403-12.
31. Vats A. Scaffolds and biomaterials for tissue engineering: a review of clinical applications. Clin. Otolaryngol Allied Sci 2003;28:165-72.
32. Ramchandani M, Robinson D. *In vito* and *in vivo* relaease of ciprofloxacin from PLGA 50:50 implants. J Controlled Release 1998;54:167-75.
33. Gao J, Niklason L, Langer R. Surface hydrolysis of Poly(glycolic acid) meshs increase the seeding density of vascular smooth muscle cells. J Biomed Mater Res 1999;42:417-24.
34. Berridge V, Tan AS. Characterization of the cellular reduction of 3-(4,5 -dimethylthiazol-2-yl)-2,5-diphenyltetrazolium bromide (MTT): Sub cellular localization, substrate dependence, and involvement of mitochondrial electron transport in MTT reduction. Arch Biochem Biophys

1993;303:474-82.

35. Amitabha B, Lorraine HK, Stefen JS, Chin CH. Impaired wound healing in mice deficient in a matricellular protein SPARC (osteonectin, BM-40). BMC Cell Biol 2001;2:15-23.
36. Schmidt HHHW, Kelm M. Methods in Nitric Oxide Research. In: Feelish M, Stamler J, editors. Chap. 33 ed. New York: John Wiley & Sons Inc; 1996. p.491-7.
37. Lee YR, Oshita Y, Tsuboi R, Ogawa H. Combination of insulin-like growth factor (IGF) -1 and IGF-binding protein-1 promotes fibroblast-embedded collagen gel contraction. Endocrinology 1996;137:5278-83.
38. Abramoff MD, Magelhaes PJ, Ram SJ. Image Processing with Image J. Biophotonics International 2004;11;36-42
39. Lee SG, An EY, Lee JB, Park J-C, Shin JW, Kim JK. Enhanced cell affinity of poly (D,L-lactic-co-glycolic acid) (50/50) by plasma treatment with beta-(1-3),(1-6) glucan. Surf Coat Technol 2007;201:5128-31.
40. Lee JE, Park J-C, Park KD, Kim YH, Suh H. *In vitro* evaluation of PEG modified polyurethanes in cellular toxicity. Biomat Res 1998;2:65-8.
41. Magnusson B, Kligman AM. The identification of contact allergens by animal assay: The guinea pig maximization test. J Invest Dermatol 1969;57:268-76.
42. Magnusson B and Kligman AM. Allergk Contact Dermatitis in the Guinea Pig: Identification of Contact Allergens, Charles C Thomas,

Springfield, IL, 1970.

43. Li W, Fan J, Chen M, Woodley DT. Mechanisms of human skin cell motility. Histol Histopathol 2004;19:1311-24.
44. Jozaki K, Marucha PT, Despins AW, Kreutzer DL. An *in vitro* model of cell migration: evaluation of vascular endothelial cell migration. Anal Biochem 1990;190:39-47.
45. McCarroll JA, Phillips PA, Kumar RK, Park S, Pirola RC, Wilson JS, et al. Pancreatic stellate cell migration: role of the phosphatidylinositol 3-kinase (PI3-kisnase) pathway. Biochem Pharmacol 2004;67:1215-25.
46. Chesrown SE, Monnier J, Visner G, Nick HS. Regulation of inducible nitric oxide synthase mRNA levels by LPS, INF-gamma, TGFbeta, and IL-10 in murine macrophage cell lines and rat peritoneal macrophages. Biochemical and Biophysical Research Communications 1994;200:126-34.
47. Singh, VK, Mehrotra S, Narayan P, Pandey CM, Agarwal SS. Modulation of autoimmune diseases by nitric oxide. Immunologic Research 2000;22:1-9.
48. Phillips JA, Vacanti CA, Bonassara LJ. Fibroblasts regulate contractile force independent of MMP activity in 3D-collagen. Biochem Biophys Res Commun 2003;312:722-5.
49. Ratner BD, Hoffman AS, Schoen FJ, Lemons JE. Biomaterials science: an introduction to materials in medicine. 2nd ed. Amsterdam: Elsevier; 2004.
50. Lerman OZ, Galiano RD, Armour M, Levine JP, Gurtner GC.

Cellular dysfunction in the diabetic fibroblast: impairment in migration, vascular endothelial growth factor production, and response to hypoxia. Am J Pathol 2003;162:303−12.

51. Clark RAF. Wound repair: overview and general considerations. In: Clark RAF, editor. The molecular and cellular biology of wound repair. 2nd ed. Plenum: New York;1996. p.3-35.
52. Raffetto JD, Mendez MV, Marien BJ, Byers HR, Phillips TJ, Park HY, et al. Changes in cellular motility and cytoskeletal actin in fibroblasts from patients with chronic venous insufficiency and in neonatal fibroblasts in the presence of chronic wound fluid. J Vasc Surg 2001;33:1233-41.
53. Elfering SL, Sarkela TM, Giulivi C. Biochemistry of mitochondrial nitric-oxide synthase. J Biol Chem 2002;277:38079-86.
54. Isenberg C, Kolmann HL. Neurocutaneous angiomatosis. Manifestation with cystic tumors. Nervenarzt 2005;76:202-4.
55. Nyska A, Lomnitski L, Maronpot R, Moomaw C, Brodsky B, Sintov A, et al. Effects of iodine on inducible nitric oxide synthase and cyclooxygenase-2 expression in sulfur mustardinduced skin. Arch Toxicol 2001;74:768-74
56. Yamasaki K, Edington HD, McClosky C, Tzeng E, Lizonova A, Kovesdi I, et al. Reversal of impaired wound repair in iNOSdeficient mice by topical adenoviral-mediated iNOS gene transfer. J Clin Invest 1998;101:967-71.
57. Michael RS, Philip AE, Frank JT, Karin K, Steven SG, Adrian B. Nitric oxide, an autocrine regulator of wound fibroblast synthetic function. J Immunol 1997;158:2375-81.

58. Stallmeyer B, Kampfer H, Kolb N, Pfeilschifter J, Frank S: The function of nitric oxide in wound repair: inhibition of inducible nitric oxide-synthase severely impairs wound reepithelialization. J Invest Dermatol 1999;113:1090-8.

59. Du M, Islam MM, Lin L, Ohmura Y, Moriyama Y, Fujimura S. Promotion of proliferation of murine BALB/C3T3 fibroblasts mediated by nitric oxide at lower concentrations. Biochem Mol Biol Int 1997; 41:625-31.

60. Witte MB, Thornton FJ, Efron DT, Barbul A. Enhancement of fibroblast collagen synthesis by nitric oxide. Nitric Oxide 2000;4:572-82.

60. Green LC, Wagner DA, Glogowski J, Skipper PL, Wishnok JS, Tannenbaum SR. Analysis of nitrate, nitrite, and [15N]nitrate in biological fluids. Anal Biochem 1982;126:131-8.

62. Bell E, Ivarsson B, Merrill C. Production of a tissue-like structure by contraction of collagen lattices by human fibroblasts of different proliferative potential in vitro. Proc. Natl. Acad. Sci. USA 1979;76:1274-78.

63. Harris AK, Stopak D, Wild P. Fibroblast traction as a mechanism for collagen morphogenesis. Nature 1981;290:249-51.

64. Stopak D, Harris AK. Connective tissue morphogenesis by fibroblast traction. I. Tissue culture observations. Dev Riol 1982;90:383-98.

65. Wald HL, Sarakinos G, Lyman MD, Mikos AG, Vacanti JP, Langer R. Cell seeding in porous transplantation devices. Biomaterials 1993; 14:270-8

Abstract in Korean

(1→3),(1→6)-β-D-glucan의 창상치유작용과 β-glucan/PLGA 혼합지지체의 세포반응성

<지도교수 박 종 철>

연세대학교 대학원 의과학과

우 연 이

베타 글루칸은 주로 버섯, 효모 등의 미생물 세포벽을 구성하는 다당류로서, 면역반응을 증가시키는 물질로 알려져 왔다. 창상치유과정은 대식세포나 섬유아세포와 같은 다양한 세포들의 상호작용을 포함하며 주로 면역 반응에 의해 조절 된다. 초기 염증 반응 과정을 담당하는 대식세포는 활성화와 함께 일련의 면역 반응을 유도한다. 대식세포는 생체 내 및 생체 외에서 여러 가지 자극물에 의해 활성화되는데, 지금까지 보고된 활성인자로 cytokine, LPS (Lipopolysaccaride) 등이 대식세포를 활성화 하여 종양이나 체내 기생체에 대항할 수 있는 면역활성을 유발시키는 가장 잠재력 있는 활성물질로 밝혀져 왔다. 본 연구에서는 흑효모로부터 추출한 (1→3),(1→6)-β-D-glucan이 섬유아세포나 지방유래줄기세포의 증식과 이동에 미치는 영향을 생체 외 실험을 통해 확인하고, 대식세포로부터 베타 글루칸의 면역기능 활성을 확인하였다. 또한 창상의 수축을 반영하는 실험실내 모델인 섬유모세포에 의한 콜라겐 젤 수축 시험을 하였다. 베타 글루칸의 생물학적 활성을 최대한 살리기 위해 이를 생분해성 고분자인 PLGA에 혼합하여 섬유아세포, 지방유래줄기세포에 각각 처리하였을 때 세포의 부착, 증식에 미치는 영향을 밝혀 창상치유를 위한 지지체

로써의 적용가능성을 확인하였다.

섬유아세포와 지방유래줄기세포의 증식과 이동 시험의 결과에서 (1→3),(1→6) 베타 글루칸은 사람의 성인 진피세포의 증식과 이동에는 효과를 갖는 반면 지방유래줄기세포의 이동에는 효과를 갖지만 증식에는 효과를 갖지 않았다. 또한 베타 글루칸은 대식세포에서 LPS에 의해 유도된 NO와 iNOS의 발현을 농도 의존적으로 억제함을 알 수 있었다. 또한 염증반응에서 또다른 주요한 요소인 COX-2와 그의 생성물인 PGE_2에 대해서도 iNOS와 유사하게 농도의존적으로 억제함이 확인되었으며 이는 염증 억제에 효과가 있음을 제시하고 있다. 창상의 수축을 반영하는 실험실내 모델인 섬유모세포에 의한 콜라겐 젤 수축도시험을 시행한 결과, 베타글루칸이 첨가된 배지를 배양액으로 사용한 경우 세포군에서 더 큰 폭으로 콜라겐 젤의 수축을 유도하였다. 이러한 결과는 (1→3), (1→6) 베타 글루칸의 적용이 창상 치유를 증진하는데 유용하다는 것을 의미한다.

베타 글루칸과 PLGA에 혼합한 지지체에 섬유아세포, 지방유래줄기세포에 각각 처리하였을 때 세포의 증식에 효과가 있었으며 생물학적 안전성 시험을 통해 독성이 없는 것으로 확인 되었다.

결론적으로, 1→3), (1→6) 베타 글루칸이 상처치유용 PLGA지지체에 함유되어 지지체의 성능을 향상시킬 가능성을 확인할 수 있었다.

핵심되는 말 : (1→3),(1→6) 베타 글루칸, 창상 치유, 섬유아세포, 지방유래줄기세포, 콜라겐, PLGA, 지지체